[3] Kimura R, Honda S, Kawasaki T, Tsuji H, Madoiwa S, Sakata Y, et al. Protein S-K196E mutation as a genetic risk factor for deep vein thrombosis in Japanese patients. Blood 2006;107:1737–8.
[4] Ikejiri M, Wada H, Sakamoto Y, Ito N, Nishioka J, Nakatani K, et al. The association of protein S Tokushima-K196E with a risk of deep vein thrombosis. Int J Hematol 2010;92:302–5.
[5] Miyata T, Kimura R, Kokubo Y, Sakata T. Genetic risk factors for deep vein thrombosis among Japanese: importance of protein S K196E mutation. Int J Hematol 2006;83: 217–23.
[6] Miyata T, Hamasaki N, Wada H, Kojima T. More on: racial differences in venous thromboembolism. J Thromb Haemost 2012;10:319–20.
[7] Miyata T, Sato Y, Ishikawa J, Okada H, Takeshita S, Sakata T, et al. Prevalence of genetic mutations in protein S, protein C and antithrombin genes in Japanese patients with deep vein thrombosis. Thromb Res 2009;124:14–8.
[8] Kimura R, Sakata T, Kokubo Y, Okamoto A, Okayama A, Tomoike H, et al. Plasma protein S activity correlates with protein S genotype but is not sensitive to identify K196E mutant carriers. J Thromb Haemost 2006;4:2010–3.
[9] Hayashi T, Nishioka J, Suzuki K. Molecular mechanism of the dysfunction of protein S(Tokushima) (Lys155– > Glu) for the regulation of the blood coagulation system. Biochim Biophys Acta 1995;1272:159–67.
[10] Liu W, Morito D, Takashima S, Mineharu Y, Kobayashi H, Hitomi T, et al. Identification of RNF213 as a susceptibility gene for moyamoya disease and its possible role in vascular development. PLoS One 2011;6:e22542.
[11] Liu W, Hitomi T, Kobayashi H, Harada KH, Koizumi A. Distribution of moyamoya disease susceptibility polymorphism p.R4810K in RNF213 in East and Southeast Asian Populations. Neurol Med Chir (Tokyo) 2012;52:299–303.
[12] Xu Q, Xu B, Zhang Y, Yang J, Gao L, Wang H, et al. Estimation of the warfarin dose with a pharmacogenetic refinement algorithm in Chinese patients mainly under low-intensity warfarin anticoagulation. Thromb Haemost 2012;108:1132–40.
[13] Abecasis GR, Auton A, Brooks LD, DePristo MA, Durbin RM, Handsaker RE, et al. An integrated map of genetic variation from 1,092 human genomes. Nature 2012;491:56–65.
[14] Ooe A, Kida M, Yamazaki T, Park SC, Hamaguchi H, Girolami A, et al. Common mutation of plasminogen detected in three Asian populations by an amplification refractory mutation system and rapid automated capillary electrophoresis. Thromb Haemost 1999;82:1342–6.
[15] Ruan C, Dai L, Su J, Wang Z. The frequency of P475S polymorphism in von Willebrand factor-cleaving protease in the Chinese population and its relevance to arterial thrombotic disorders. Thromb Haemost 2004;91:1257–8.

Wanyang Liu
Department of Health and Environmental Sciences, Kyoto University Graduate School of Medicine, Kyoto, Japan
Department of Occupational and Environmental Health, School of Public Health, China Medical University, Shenyang, China

Tong Yin
Yang Li
Bin Xu
Jie Yang
Hongjuan Wang
Institute of Geriatric Cardiology, General Hospital of Chinese People's Liberation Army, Beijing, China

Hiroko Okuda
Kouji H. Harada
Akio Koizumi
Department of Health and Environmental Sciences, Kyoto University Graduate School of Medicine, Kyoto, Japan

Xinping Fan
Department of Molecular Pathogenesis, National Cerebral and Cardiovascular Center, Suita, Osaka, Japan
Department of Clinical Laboratory, Beijing Chaoyang Hospital, Capital Medical University, Beijing, China

Toshiyuki Miyata
Department of Molecular Pathogenesis, National Cerebral and Cardiovascular Center, Suita, Osaka, Japan
Corresponding author. Tel.: +81 6 6833 5012; fax: +81 6 6835 1176.
E-mail address: miyata@ri.ncvc.go.jp.

27 March 2013

Hindawi Publishing Corporation
Case Reports in Medicine
Volume 2013, Article ID 270419, 6 pages
http://dx.doi.org/10.1155/2013/270419

Case Report

Budd-Chiari Syndrome with Multiple Thrombi due to a Familial Arg42Ser Mutation in the Protein C Gene

Jun Muratsu,[1] Atsuyuki Morishima,[1] Kazuhiro Mizoguchi,[2] Keiji Ataka,[2] Hiroshi Yamamoto,[3] Xinping Fan,[4] Toshiyuki Miyata,[4] and Katsuhiko Sakaguchi[1]

[1] *Department of Nephrology and Hypertension, Sumitomo Hospital, 5-3-20 Nakanoshima, Kitaku, Osaka 530-0005, Japan*
[2] *Department of Cardiovascular Surgery, Sumitomo Hospital, 5-3-20 Nakanoshima, Kitaku, Osaka 530-0005, Japan*
[3] *Department of Radiology, Sumitomo Hospital, 5-3-20 Nakanoshima, Kitaku, Osaka 530-0005, Japan*
[4] *Department of Molecular Pathogenesis, National Cerebral and Cardiovascular Center, 5-7-1 Fujishirodai, Suita, Osaka 565-8565, Japan*

Correspondence should be addressed to Jun Muratsu; jm27252725@yahoo.co.jp

Received 22 April 2013; Accepted 9 September 2013

Academic Editor: Yasuhiko Sugawara

A 34-year-old Japanese woman was admitted to our hospital complaining of developing bilateral pedal edema. Imaging studies led to a diagnosis of Budd-Chiari syndrome combined with internal jugular vein thrombus. We investigated the cause of thrombosis and found that the anticoagulant activity of protein C was decreased. Genetic analysis showed the presence of a c.125C>A (Arg42Ser) substitution in the protein C gene (*PROC*) of the proband, which generates an Arg42Ser mutation that replaces the scissile bond Arg42-Ala43 normally cleaved by a furin-like processing protease. Her father and younger brother also carried this mutation, although they had no evidence of thrombosis.

1. Introduction

Budd-Chiari syndrome is defined as any pathophysiologic process, such as thrombosis, that results in an interruption or diminution of the normal flow of blood from the liver [1]. One cause of this syndrome is a deficiency in protein C [2–4], a precursor of a vitamin K-dependent serine protease that plays an important role in the regulation of blood coagulation [5–7]. Heterozygous protein C deficiency is inherited in an autosomal dominant fashion, and hereditary deficiency in this protein is associated with a high risk of thrombotic disease [8]. A c.125C>A change in the protein C gene (*PROC*) is designated protein C Osaka 10. This mutation had been reported in only one case so far [9]. Although some cases of Budd-Chiari syndrome have been reported to be caused by hereditary protein C deficiency, genetic analysis of family members was not investigated.

To our knowledge, the present study represents the first case report describing Budd-Chiari syndrome combined with multiple thrombotic lesions and genetic analysis of family members.

2. Case Report

A 34-year-old Japanese woman was admitted to our hospital complaining of a weight gain of up to 15 kg and increased bilateral pedal edema over the preceding 3 weeks. She did not have a history of these symptoms and was not taking any medications. On admission, her pulse rate was 84 beats/min, her blood pressure was 130/84 mmHg, and her body temperature, 36.7°C. Her consciousness was alert, her bulbar conjunctiva were not icteric, and the palpebral conjunctiva were not pale. No respiratory rales or heart murmurs were noted on auscultation. Palpation revealed hepatosplenomegaly and ascites with no enlargement of the thyroid gland. Neurological abnormalities, jaundice, or palmar erythema was not evident. However, bilateral pedal edema was observed.

Laboratory data acquired upon admission are shown in Table 1. Alanine aminotransferase (ALT) (46 IU/L) and D-dimer (1.40 μg/mL) were slightly elevated. Her chest X-ray and echocardiogram were normal, but carotid ultrasonography showed a thrombus of the right internal jugular

Table 1: Laboratory test values of the proband upon admission.

Complete blood count	
White blood cell count	6,600/μL
Red blood cell count	$396 \times 10^4/\mu$L
Hemoglobin	12.4 g/dL
Hematocrit	37.6%
Platelets	$16.0 \times 10^4/\mu$L
Blood biochemistry	
Aspartate aminotransferase	29 IU/L
Alanine aminotransferase	46 IU/L
Alkaline phosphatase	175 IU/L
Lactate dehydrogenase	190 IU/L
γ-GTP	39 IU/L
Total bilirubin	0.8 mg/dL
Creatine phosphokinase	79 IU/L
Total cholesterol	299 mg/dL
Triglyceride	104 mg/dL
HDL-cholesterol	72 mg/dL
LDL-cholesterol	195 mg/dL
Sodium	143 mEq/L
Chloride	108 mEq/L
Potassium	3.9 mEq/L
Uric acid	3.1 mg/dL
Blood urea nitrogen	8 mg/dL
Creatinine	0.57 mg/dL
Total protein	5.1 g/dL
Albumin	3.5 g/dL
C-reactive protein	0.20 mg/dL
Hemoglobin A1c	5.6%
Thyroid-stimulating hormone	1.72 μIU/mL
Thyroxine, free (fT4)	0.8 pg/mL
Thyroxine, free (fT3)	2.0 pg/mL
BNP	21.1 pg/mL
Coagulation	
APTT	32.5 s
PT-INR	1.06
D-dimer	1.40 μg/mL
Immunochemistry	
Immunoglobulin G	320 mg/dL
Immunoglobulin A	71 mg/dL
Immunoglobulin M	114 mg/dL
Immunoglobulin E	17.6 IU/mL
Complement titer (CH50)	52.8 U/mL
Complement C3	111 mg/dL
Complement C4	37 mg/dL
Antinuclear antibody	<40
Lupus anticoagulant	(−)
HBs antigen	(−)
HCV-antibody	(−)
<ELISA>	
MPO-ANCA	93 EU
PR3-ANCA	<10 EU
Urinalysis	
pH	7.0
Specific gravity	1.010
Glucose	(−)
Protein	(−)
Cast	(−)
Erythrocytes	1–5/HPF
Leukocytes	1–5/HPF

Abbreviations: γ-GTP: gamma-glutamyl transpeptidase; HDL cholesterol: high-density lipoprotein-cholesterol; LDL cholesterol: low-density lipoprotein cholesterol; PR3-ANCA: proteinase-3 antineutrophil cytoplasmic antibody; MPO-ANCA: myeloperoxidase antineutrophil cytoplasmic antibody; APTT: activated partial thromboplastin time; BNP: B-type natriuretic peptide; PT-INR: prothrombin time-international normalized ratio.

vein (Figure 1(a)). Blood flow in the right internal jugular vein was maintained and did not require immediate treatment. Abdominal ultrasonography and computed tomography (CT) showed hepatomegaly, ascites, gallbladder wall thickening, and a thrombus within the intrahepatic portion of the inferior vena cava. Abdominal magnetic resonance imaging (MRI) revealed a region of high-intensity, which suggested the presence of a thrombus within the inferior vena cava (Figure 1(b)). Abdominal-pelvic CT and MRI analyses did not detect tumors. The presence of right pleural effusion and dilatation of an azygos vein were evident in CT images acquired following the injection of contrast medium (Figure 1(c)). Venous angiography revealed a thrombus within the inferior vena cava at its outlet that extended to the right atrium and was accompanied by intrahepatic collaterals (Figures 2(a) and 2(b)). This patient was therefore diagnosed with Budd-Chiari syndrome.

Based on the results of a previous study, we expected that percutaneous transluminal angioplasty (PTA), a minimally invasive procedure, would result in a favorable outcome [10]. We performed PTA with stent implantation (LUMINEXX 14 × 80 mm) and successful balloon dilatation (OPTA Pro 10 × 40 mm) from the outlet of the inferior vena cava to the right atrium (Figures 2(c) and 2(d)). The pressure of the inferior vena cava decreased after PTA from 25 mmHg to 16 mmHg. Although we prepared the operation for a case of pulmonary embolism, PTA was completed without any complications. We started treatment by administering intravenous heparin sodium (10,000 units/day). Heparin sodium infusion was discontinued 2 days after PTA, and the patient's postoperative course was uneventful. Abdominal CT during injection of contrast medium was performed on postoperative day 10 and showed the patency of the inferior vena cava. Abdominal ultrasonography showed that hepatomegaly, ascites, and gallbladder wall thickening were diminished. Bilateral pedal edema was dramatically alleviated after 14 days.

We examined protein C anticoagulant activity and it was decreased to 44% (normal: 64%–146%), contributing to thrombogenesis. Protein C anticoagulant activity was decreased in her father (61%) and younger brother (62%) (Table 2). While the medical histories of her younger brother and father were not informative, her younger brother had

TABLE 2: Analysis of clotting factors.

	Age	Gender	Arg42Ser mutation	Protein C anticoagulant activity (%)	Protein C antigen (%)	Protein S activity (%)	D-dimer (mg/mL)
Patient	35	Female	+	44	46*	85	1.4
Younger brother	31	Male	+	62	48*	118	0.22
Father	60	Male	+	61	128	147	0.26
Mother	61	Female	−	105	97	98	0.22

*Administration of warfarin.

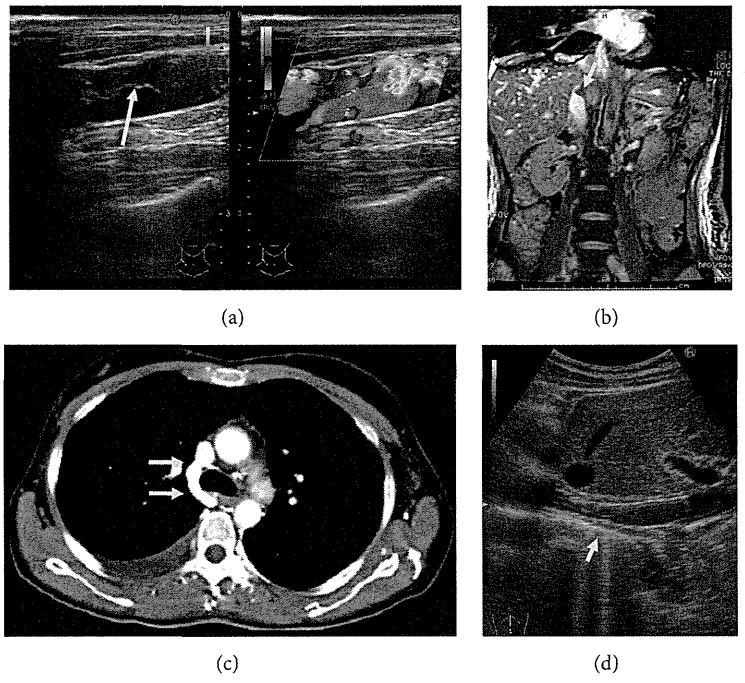

FIGURE 1: Imaging studies. (a) Carotid ultrasonography shows a thrombus of the right internal jugular vein indicated by the arrow. Blood flow in the right internal jugular vein was maintained. (b) Abdominal MRI first imaging employing steady state acuisition (FIESTA) reveals a high-intensity signal emanating from the intrahepatic portion of the inferior vena cava (arrow), which suggested thrombus. (c) Thoracic CT during injection of contrast medium reveals right pleural effusion and dilatation of an azygos vein at the arrows. (d) Abdominal Doppler ultrasonography shows complete patency (arrow) and no ectopia of the stent. This image was acquired 16 months after the patient was admitted.

been suffering for several years from idiopathic recurrent chest pain.

To determine whether or not the patient and her family members harbored *PROC* mutations, we performed genetic analyses after we obtained informed written consent. Genomic DNA was isolated from blood samples using a QIAamp DNA Blood MiniKit kit (Qiagen). All exons and flanking intronic regions of *PROC* were amplified using polymerase chain reaction (PCR) and then sequenced in both sense and antisense strands using an ABI Prism BigDye Terminator v3.1 Cycle Sequencing kit (Applied Biosystems) [11]. Primer sequences are available on request. A c.125C>A change that encodes an Arg42Ser mutation was identified in the patient. Arg42 is located at the cleavage site recognized by the furin-like protease that normally processes preproprotein C to its mature form.

This mutation was also identified in the patient's father and younger brother, whereas the sequence of her mother's DNA in this region was found to be wild-type (Figure 3). Although her younger brother did not have evidence of thrombosis, his idiopathic recurrent chest pain may be shown by pulmonary embolism due to microscopic thrombosis. And he desired administration of warfarin. Warfarin (3–6 mg/day orally) was given to the patient and younger brother according to the levels of prothrombin time-international normalized ratio (maintaining between 2.0 and 2.5). Abdominal Doppler ultrasonography, which was performed during a follow-up visit to the outpatient clinic 16 months after the procedure, showed complete patency and no ectopia of the stent (Figure 1(d)). Carotid ultrasonography showed that blood flow in the right internal jugular vein was maintained.

3. Discussion

We describe here a patient with Budd-Chiari syndrome with multiple venous thrombi caused by an Arg42Ser mutation

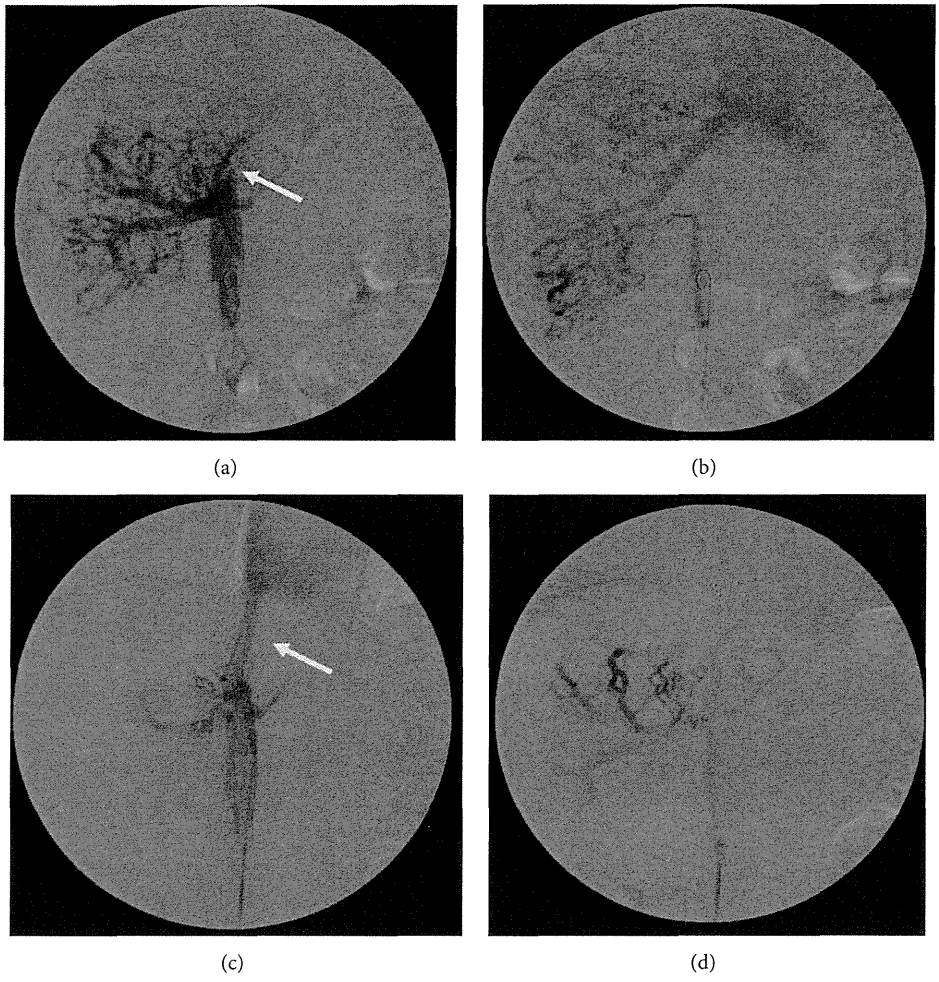

FIGURE 2: Angiography. ((a), (b)) Angiography reveals a thrombus in the inferior vena cava, which extends from its outlet to the right atrium. The intrahepatic collaterals are also shown. A portion of thrombus is indicated by the arrow. ((c), (d)) We performed PTA with stent implantation (LUMINEXX 14 × 80 mm) and successful balloon dilatation (OPTA Pro 10 × 40 mm) of the inferior vena cava at its outlet to the right atrium. The arrow points to the the stent.

in *PROC*. Her father and younger brother also carried this mutation; however, they were free of detectable thrombosis. Her mother was genetically unaffected.

Budd-Chiari syndrome is defined as any pathophysiologic process that results in an interruption or diminution of the normal flow of blood out of the liver. This presentation is uncommon, often dramatic illness characterized by abdominal pain, ascites, hepatomegaly and a poor prognosis [1]. The diagnosis can be established noninvasively by ultrasonography with Doppler studies, CT scan, or magnetic resonance angiography (MRI angiography) [12–14]. Treatment depends upon the cause, the anatomic location, and extent of the thrombotic process [15]. The etiology of Budd-Chiari syndrome, a rare disorder, is varied, and its cause remains unknown in most patients [16]. Analysis of 157 patients with Budd-Chiari syndrome in Japan revealed that 141 were idiopathic, 2 were deficient in protein C, 2 were deficient in protein S, and 1 was deficient in antithrombin [17]. Protein C deficiency is one of the causes of Budd-Chiari syndrome [2–4].

Protein C is the precursor of a vitamin K-dependent serine protease that plays an important role in the regulation of blood coagulation [5–7]. The observed molecular mass of protein C is approximately 62 kDa, accounted for by one light chain (21 kDa) and one heavy chain (41 kDa), which are connected by a disulfide bridge. The primary effect of activated protein C is to inactivate coagulation factors Va and VIIIa, which are necessary for the efficient generation of thrombin and the activation of factor X. Congenital protein C deficiency is most often transmitted as an autosomal dominant trait with varying degrees of penetrance [18]. Heterozygous protein C deficiency is an important independent risk factor for the development of deep vein thrombosis, [19] characterized by recurrent venous thrombosis. In this case, c.125C>A *PROC* mutation was identified in the proband, where CGT encoding Arg42 at the furin-like processing enzyme cleavage site was changed to AGT encoding Ser. This mutation abolishes the cleavage site required for production of mature protein C molecule [9]. In this mutation, the specificity of the processing protease would be shifted to a Lys-Ser bond to

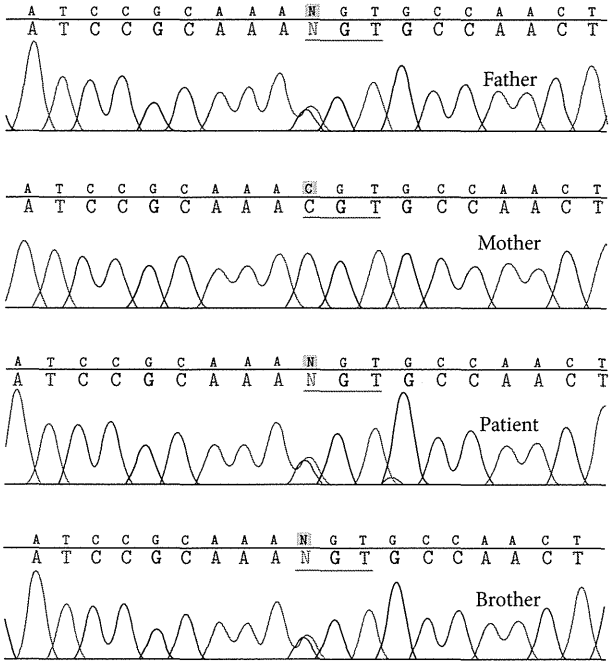

FIGURE 3: DNA sequence analysis. A c.125C>A substitution in the *PROC* sequence of the proband. The CGT encoding Arg42 at the processing cleavage site, which is recognized by the processing enzyme, is changed to AGT, encoding Ser. This mutation was also identified in her father and her younger brother but not in her mother.

produce mutant protein C with loss of anticoagulant activity. Protein C Osaka 10 showed normal amidolytic activity and a normal protein C antigen level; however, it had an anticoagulant activity of only about 50% compared to that of the wild-type protein. This mutation is characterized as type 2 protein C deficiency. In this case, protein C antigen of the patient and her younger brother was decreased by administration of warfarin (Table 2).

In a study of 173 patients with deep vein thrombosis, 55 (32%) were found to carry mutations in genes encoding protein S, protein C, and antithrombin [11]. However, deficiency of protein C occurs in a variety of other conditions, such as severe liver disorders, the nephrotic syndrome, acute respiratory distress, and postoperative states [20], suggesting the importance of extending investigations of *PROC* particularly to patients suffering from multiple thrombi. The frequency of heterozygous protein C deficiency may be as high as 1/200 to 1/500 in healthy adults; however, those affected do not exhibit thrombotic manifestations [21, 22]. This study also indicates that other unidentified factors may play an important role in the clinical signs of thrombosis formation.

The patient, her father, and younger brother described here express Protein C Osaka 10. However, her father and younger brother showed no detectable thrombi. The implementation of primary prophylaxis with aspirin, heparin, or warfarin is often considered in known familial cases. Anticoagulant prophylaxis is given to all patients who develop a venous clot regardless of the underlying cause. Patients with protein C deficiency are at increased risk of recurrent venous thromboembolic events. Long term anticoagulation therapy using warfarin may be considered in these patients [23]. Therefore, we believe that familial screening for *PROC* mutations could avoid new thrombotic complications as well as improving the long term prognosis of the patients with Budd-Chiari syndrome caused by protein C deficiency.

We suggest a hypothesis to account for the absence of detectable thrombosis in our patient's family members, these individuals harbored the same mutation as our patient with a concomitant decrease in protein C activity. The hypothesis maintains that elevated levels of total cholesterol may be a risk factor for venous thromboembolism (VTE). Studies on the association between lipid profile and VTE are inconsistent, with some reporting that total cholesterol is the risk factor [24], while others report that lipid levels do not influence the risk of VTE; however, the levels of LDL are significantly associated with unprovoked VTE as revealed by univariate analysis [25]. Further, statins can prevent VTE [26]. The levels of total cholesterol and LDL cholesterol in our patient (total cholesterol, 299 mg/dL, LDL cholesterol, 195 mg/dL) were higher than those of her younger brother (total cholesterol, 234 mg/dL, LDL cholesterol; 161 mg/dL) and father (total cholesterol, 200 mg/dL, LDL cholesterol, 99 mg/dL). Moreover, we noted no recurrence of thrombosis after statins were administered to our patient.

In summary, we describe here a case of Budd-Chiari syndrome with multiple venous thrombi caused by an Arg42Ser mutation in *PROC* and in two of three of her family members without detectable thrombosis. Thus, the patient's brother and father did not experience thrombotic events, even though they harbored the same mutation with a concomitant decrease in protein C activity. Further, the difference between the patient's complicated thrombosis and family members with no thrombosis, even though they all harbor the same *PROC* mutation, may be associated with lipid levels. Therefore, the contribution of this mutation to thrombogenicity remains to be determined.

Conflict of Interests

The authors state that they have no conflict of interests.

References

[1] K. V. N. Menon, V. Shah, and P. S. Kamath, "Current concepts the Budd-Chiari syndrome," *The New England Journal of Medicine*, vol. 350, no. 6, pp. 578–585, 2004.

[2] S. Sugano, T. Suzuki, H. Makino et al., "Budd-Chiari syndrome attributed to protein C deficiency," *The American Journal of Gastroenterology*, vol. 91, no. 4, pp. 777–779, 1996.

[3] A. Majluf-Cruz, R. H. Monroy, L. S. García, and J. Labardini-Méndez, "The incidence of protein C deficiency in thrombosis-related portal hypertension," *The American Journal of Gastroenterology*, vol. 91, no. 5, pp. 976–980, 1996.

[4] M. Bourliere, Y. P. Le Treut, D. Arnoux et al., "Acute Budd-Chiari syndrome with hepatic failure and obstruction of the inferior vena cava as presenting manifestations of hereditary protein C deficiency," *Gut*, vol. 31, no. 8, pp. 949–952, 1990.

[5] W. Kisiel, L. H. Ericsson, and E. W. Davie, "Proteolytic activation of protein C from bovine plasma," *Biochemistry*, vol. 15, no. 22, pp. 4893–4900, 1976.

[6] C. T. Esmon, "Protein-C: biochemistry, physiology, and clinical implications," *Blood*, vol. 62, no. 6, pp. 1155–1158, 1983.

[7] J. Stenflo, "A new vitamin K dependent protein: purification from bovine plasma and preliminary characterization," *Journal of Biological Chemistry*, vol. 251, no. 2, pp. 355–363, 1976.

[8] R. M. Bertina, A. W. Broekmans, I. K. van der Linden, and K. Mertens, "Protein C deficiency in a Dutch family with thrombotic disease," *Thrombosis and Haemostasis*, vol. 48, no. 1, pp. 1–5, 1982.

[9] T. Miyata, Y.-Z. Zheng, T. Sakata, and H. Kato, "Protein C Osaka 10 with aberrant propeptide processing: loss of anticoagulant activity due to an amino acid substitution in the protein C precursor," *Thrombosis and Haemostasis*, vol. 74, no. 4, pp. 1003–1008, 1995.

[10] N. C. Fisher, I. McCafferty, M. Dolapci et al., "Managing Budd-Chiari syndrome: a retrospective review of percutaneous hepatic vein angioplasty and surgical shunting," *Gut*, vol. 44, no. 4, pp. 568–574, 1999.

[11] T. Miyata, Y. Sato, J. Ishikawa et al., "Prevalence of genetic mutations in protein S, protein C and antithrombin genes in Japanese patients with deep vein thrombosis," *Thrombosis Research*, vol. 124, no. 1, pp. 14–18, 2009.

[12] S. Gupta, S. Barter, and G. W. L. Phillips, "Comparison of ultrasonography, computed tomography and 99mTc liver scan in diagnosis of Budd-Chiari syndrome," *Gut*, vol. 28, no. 3, pp. 242–247, 1987.

[13] P. Soyer, A. Rabenandrasana, J. Barge et al., "MRI of Budd-Chiari syndrome," *Abdominal Imaging*, vol. 19, no. 4, pp. 325–329, 1994.

[14] A. C. Friedman, P. Ramchandani, M. Black, D. F. Caroline, P. D. Radecki, and P. Heeger, "Magnetic resonance imaging diagnosis of Budd-Chiari syndrome," *Gastroenterology*, vol. 91, no. 5, pp. 1289–1295, 1986.

[15] D.-C. Valla, "The diagnosis and management of the Budd-Chiari syndrome: consensus and controversies," *Hepatology*, vol. 38, no. 4, pp. 793–803, 2003.

[16] R. G. Parker, "Occlusion of the hepatic veins in man," *Medicine*, vol. 38, pp. 369–402, 1959.

[17] H. Okuda, H. Yamagata, H. Obata et al., "Epidemiological and clinical features of Budd-Chiari syndrome in Japan," *Journal of Hepatology*, vol. 22, no. 1, pp. 1–9, 1995.

[18] M. H. Horellou, J. Conard, R. M. Bertina, and M. Samama, "Congenital protein C deficiency and thrombotic disease in nine French families," *British Medical Journal*, vol. 289, no. 6454, pp. 1285–1287, 1984.

[19] E. G. Bovill, K. A. Bauer, J. D. Dickerman, P. Callas, and B. West, "The clinical spectrum of heterozygous protein C deficiency in a large New England kindred," *Blood*, vol. 73, no. 3, pp. 712–717, 1989.

[20] R. L. Nachman and R. Silverstein, "Hypercoagulable states," *Annals of Internal Medicine*, vol. 119, no. 8, pp. 819–827, 1993.

[21] J. Miletich, L. Sherman, and G. Broze Jr., "Absence of thrombosis in subjects with heterozygous protein C deficiency," *The New England Journal of Medicine*, vol. 317, no. 16, pp. 991–996, 1987.

[22] R. C. Tait, I. D. Walker, P. H. Reitsma et al., "Prevalence of protein C deficiency in the healthy population," *Thrombosis and Haemostasis*, vol. 73, no. 1, pp. 87–93, 1995.

[23] N. A. Goldenberg and M. J. Manco-Johnson, "Protein C deficiency," *Haemophilia*, vol. 14, no. 6, pp. 1214–1221, 2008.

[24] T. Kawasaki, J.-I. Kambayashi, H. Ariyoshi, M. Sakon, E. Suehisa, and M. Monden, "Hypercholesterolemia as a risk factor for deep-vein thrombosis," *Thrombosis Research*, vol. 88, no. 1, pp. 67–73, 1997.

[25] I. M. van Schouwenburg, B. K. Mahmoodi, R. T. Gansevoort et al., "Lipid levels do not influence the risk of venous thromboembolism. Results of a population-based cohort study," *Thrombosis and Haemostasis*, vol. 108, no. 5, pp. 923–929, 2012.

[26] A. Perez and J. R. Bartholomew, "Statins can prevent VTE, but more study is needed," *Cleveland Clinic Journal of Medicine*, vol. 77, no. 3, pp. 191–194, 2010.

The Integrin-Linked Kinase-PINCH-Parvin Complex Supports Integrin αIIbβ3 Activation

Shigenori Honda[1*], Hiroko Shirotani-Ikejima[1], Seiji Tadokoro[2], Yoshiaki Tomiyama[2,3], Toshiyuki Miyata[1]

1 Department of Molecular Pathogenesis, National Cerebral and Cardiovascular Center, Suita, Japan, **2** Department of Hematology and Oncology, Osaka University.Graduate School of Medicine, Suita, Osaka, Japan, **3** Department of Blood Transfusion, Osaka University Hospital, Suita, Osaka, Japan

Abstract

Integrin-linked kinase (ILK) is an important signaling regulator that assembles into the heteroternary complex with adaptor proteins PINCH and parvin (termed the IPP complex). We recently reported that ILK is important for integrin activation in a Chinese hamster ovary (CHO) cell system. We previously established parental CHO cells expressing a constitutively active chimeric integrin (αIIbα6Bβ3) and mutant CHO cells expressing inactive αIIbα6Bβ3 due to ILK deficiency. In this study, we further investigated the underlying mechanisms for ILK-dependent integrin activation. ILK-deficient mutant cells had trace levels of PINCH and α-parvin, and transfection of ILK cDNA into the mutant cells increased not only ILK but also PINCH and α-parvin, resulting in the restoration of αIIbα6Bβ3 activation. In the parental cells expressing active αIIbα6Bβ3, ILK, PINCH, and α-parvin were co-immunoprecipitated, indicating the formation of the IPP complex. Moreover, short interfering RNA (siRNA) experiments targeting PINCH-1 or both α- and β-parvin mRNA in the parent cells impaired the αIIbα6Bβ3 activation as well as the expression of the other components of the IPP complex. In addition, ILK mutants possessing defects in either PINCH or parvin binding failed to restore αIIbα6Bβ3 activation in the mutant cells. Kindlin-2 siRNA in the parental cells impaired αIIbα6Bβ3 activation without disturbing the expression of ILK. For CHO cells stably expressing wild-type αIIbβ3 that is an inactive form, overexpression of a talin head domain (THD) induced αIIbβ3 activation and the THD-induced αIIbβ3 activation was impaired by ILK siRNA through a significant reduction in the expression of the IPP complex. In contrast, overexpression of all IPP components in the αIIbβ3-expressing CHO cells further augmented THD-induced αIIbβ3 activation, whereas they did not induce αIIbβ3 activation without THD. These data suggest that the IPP complex rather than ILK plays an important role and supports integrin activation probably through stabilization of the active conformation.

Citation: Honda S, Shirotani-Ikejima H, Tadokoro S, Tomiyama Y, Miyata T (2013) The Integrin-Linked Kinase-PINCH-Parvin Complex Supports Integrin αIIbβ3 Activation. PLoS ONE 8(12): e85498. doi:10.1371/journal.pone.0085498

Editor: Maddy Parsons, King's College London, United Kingdom

Received August 3, 2013; **Accepted** December 5, 2013; **Published** December 23, 2013

Funding: This work was supported in part by grants from the Ministry of Health, Labor, and Welfare of Japan; and from the Ministry of Education, Culture, Sports, Science, and Technology of Japan. The funders had no role in study design, data collection and analysis, decision to publish, or preparation of the manuscript.

Competing interests: The authors have declared that no competing interests exist.

* E-mail: shige@ncvc.go.jp

Introduction

Cell adhesions are critical for hemostasis processes composed of interactions between vessel walls, platelets and coagulation-related proteins. During these processes, cells react with several elements such as extracellular matrix (ECM) proteins and cell surface receptors. As one of the main elements, an integrin family is known to play a key role in cell-ECM interactions. Integrins, transmembrane glycoprotein adhesion receptors, are composed of α and β subunits and are linked non-covalently. Both subunits include long extracellular domains, transmembrane domains, and short cytoplasmic domains. There are at least two conformational states of integrin presenting low affinity (inactive) or high affinity (active) against its ligands and this heterodimeric receptor acts as a bidirectional signaling transducer. The binding of the cytoplasmic proteins such as talin and kindlins to the integrin β cytoplasmic domain upregulates the ligand-binding affinity of integrin (inside-out signaling). In contrast, ligand binding to integrins and the subsequent clustering of ligand-bound integrins result in intracellular molecular rearrangements such as focal adhesion formation and cell spreading (outside-in signaling) [1].

αIIbβ3, a major integrin expressed on platelets, is critical for platelet aggregation mediated by bindings of fibrinogen and von Willebrand factor. Since inside-out signaling pathways of αIIbβ3 induce striking conformational changes between inactive and active states, the activation processes of αIIbβ3 have been extensively investigated [2]. Talin, a cytoskeletal protein consisting of an N-terminal head and a C-terminal rod,

has been well characterized as an integrin activator [3,4]. The talin head domain (THD) contains four subdomains: F0, F1, F2, and F3. The F3 domain itself can bind to the β3 cytoplasmic domain and exert αIIbβ3 activation [5]. Other subdomains also have important roles in the activation [6-8]. The kindlin family members (kindlin-1, -2, and -3), which are focal adhesion proteins, have recently been proven to be critical for integrin activation [9,10]. Kindlin-1 and -2 are widely expressed and kindlin-3 expression is restricted mainly to hematopoietic cells [11]. Several studies suggest that the binding of talin and kindlins to the integrin β3 cytoplasmic domain is pivotal for the final step in the inside-out activation of αIIbβ3. Moreover, since kindlins synergistically augment talin-dependent αIIbβ3 activation, they act as a co-activator of talin [12,13]. However, regulatory molecules other than talin and kindlins necessary to αIIbβ3 activation remain to be fully clarified.

Since platelets are inadequate for gene manipulation, the CHO cell system has been used to study essential regulators of integrin αIIbβ3 function. For example, αIIbβ3-expressing CHO cells contributed to the elucidation of the functional importance of kindlin-1 and -2 as co-activators and of THD as a direct activator of integrin [10,12]. It was also shown that the Rap1-GTP-interacting adaptor molecule promotes talin-dependent integrin activation in the CHO cell system [14]. A chimeric integrin, αIIbα6Aβ3β1 or αIIbα5β3, expressed on CHO cells having the extracellular and transmembrane domains of αIIbβ3 connected to the cytoplasmic domains of α6Aβ1or α5β3 has been constitutively active on CHO cells but susceptible to integrin regulatory proteins [15]. Several integrin regulatory proteins including H-ras, PEA-15, CD98, and talin were characterized in this cell system [15-18]. Thus, the CHO cell system has been utilized to analyze the mechanisms by which integrin function is regulated.

Integrin-linked kinase (ILK) was originally identified as a serine/threonine kinase associated with integrin β1 and β3 cytoplasmic domains. It consists of three domains: an N-terminal ankyrin repeat domain, a putative pleckstrin homology domain, and a C-terminal kinase domain [19]. Many studies have shown that ILK is widely expressed and involved in interactions between integrins, cytoskeletal proteins, and signaling molecules. A deficiency or aberrant function of ILK resulted in the impairment of adhesion, spreading, migration, proliferation, and survival of the cells [20]. ILK seems to have two functions: that of a scaffold protein and that of a protein kinase, whereas the kinase activity is controversial [21,22]. At focal adhesion sites, ILK forms a heterotrimeric complex composed of the adaptor proteins PINCH and parvin [23-28]. PINCH consists of two members, PINCH-1 and -2, each of which consists of five LIM domains. PINCH-1 and -2 are ubiquitously expressed in mammalian tissues and show overlapping expression in many tissues. Parvin comprises three members, α-, β-, and γ-parvin, and contains N-terminal nuclear localization sequences and two calponin homology domains. In mammalian tissues, α- and β-parvin are ubiquitously expressed but γ-parvin is expressed mainly in hematopoietic tissues. These adaptor proteins are known to directly bind to several cytoplasmic proteins including Nck2 for PINCH and filamentous actin for parvin [25,29]. The ankyrin repeat domain of ILK binds to PINCH and the kinase domain binds to parvin. ILK interacts directly or indirectly with several other cytoskeletal and signaling proteins and exerts diverse roles in different tissues [30].

In our previous study, we identified ILK as a molecule important for integrin activation, using an expression cloning system as follows. First, we established CHO cells expressing constitutively active integrin αIIbα6Bβ3 whose αIIb cytoplasmic domain we replaced by that of integrin α6B (parental cells). Next we obtained mutant cells with inactive integrin using genome-wide mutagenesis, and finally isolated an ILK cDNA was isolated as a factor that complements the function of inactive αIIbα6Bβ3 in mutant cells by expression cloning [31]. Although the role of ILK at focal adhesion sites has been well studied, there are only a few reports on the involvement of ILK in integrin activation [32,33]. In the present study, we further investigated the mechanisms by which ILK regulates integrin activation in the CHO cell system.

Materials and Methods

Plasmids

Human wild-type (WT) αIIb and β3 subcloned into expression plasmid pcDNA3 (Invitrogen, San Diego, CA) were provided by Drs P. Newman and G. White (Blood Research Institute, Blood Center of Wisconsin, Milwaukee, WI). pRKHA, including full-length mouse talin-1 was a gift from Dr K. Yamada (NIH, Bethesda, MD). The N-terminal head region (residues 1-433) of talin-1 was constructed by polymerase chain reaction (PCR) and subcloned into green fluorescence protein (GFP) containing vector pEGFP-N1 to make a fusion protein of THD with GFP (THD-GFP) (Clontech, Mountain View, CA). Mouse α-parvin cDNA and mouse PINCH-1 cDNA (Thermo Scientific Open Biosystems, Lafayette, CO) were amplified by PCR and then were subcloned into expression plasmids, pcDNA3.1 (Invitrogen) for α-parvin and pBApo-CMV Pur DNA (Takara Bio, Shiga, Japan) for PINCH-1. pcDNA3-αIIbα6B was created using PCR-based mutagenesis as previously described [31]. Nucleotide and amino acid numbers begin with the start codon (ATG) and the first Met residue, respectively. The full length of rat ILK cDNA was amplified by PCR then subcloned into pcDNA3 and GFP-encoding plasmid pAcGFP1-Hyg-C1 to make a fusion protein of ILK with GFP (GFPILK-WT) (Clontech). Three point mutations (H99D/F109A/W110A) in the ankyrin repeat domain of ILK were introduced into pAcGFP1-Hyg-C1 to make a fusion protein of the ILK mutant with GFP (GFPILK-H99D/F109A/W110A). Two point mutations (M402A/K403A) in the ILK kinase domain were introduced in pAcGFP1-Hyg-C1 to make a fusion protein of the ILK mutant with GFP (GFPILK-M402/K403A). The ILK mutant (H99D/F109A/W110A) was designed to disrupt the PINCH binding based on the crystal structure of a complex of the ankyrin repeat domain of ILK with the LIM1 domain of PINCH, PDB 3F6Q [34]. The ILK mutant (M402A/K403A) was designed to disrupt the parvin binding as previously reported [35]. Expression plasmid pCMV-SPORT6, containing full-length mouse kindlin-2 (Thermo Scientific Open Biosystems) was obtained. All PCR-generated DNA inserts were verified by

sequencing using a BigDye Terminator Cycle Sequencing Kit (Applied Biosystems, Foster City, CA).

Cell Cultures

CHO-K1 cells from ATCC were cultured in DMEM supplemented with 10% fetal bovine serum and 1% non-essential amino acids (Sigma-Aldrich, St. Louis, MO). CHO cells stably expressing constitutively active αIIbα6Bβ3 (parental cells) were previously established [31]. CHO-K1 cells were cotransfected with pcDNA3-αIIbα6B and pcDNA3-β3 using Lipofectamine 2000 (Invitrogen) and selected with 1 mg/ml G418 (Nacalai Tesque, Kyoto, Japan). G418-resistant cells expressing αIIbα6Bβ3 were cloned to isolate parental cells by a limiting dilution method. ILK-deficient mutant cells, which result in its inactive form from active αIIbα6Bβ3 (mutant cells), were previously established by the introduction of random mutations into the parental cells using a chemical mutagen, ethyl methane sulfonate (EMS) [31]. For αIIbβ3-expressing CHO cells, pBApo-CMV Pur DNA-αIIb and pcDNA3-β3 were cotransfected into CHO-K1 cells by Lipofectamine 2000. After selection with 12 μg/ml puromycin (Clontech) and 1 mg/ml G418, clones expressing αIIbβ3 were established by the limiting dilution method.

Flow cytometry

Flow cytometry analyses were performed as previously described [31]. Cells suspended in Tyrode's buffer containing 1.5 mM $CaCl_2$, 1 mM $MgCl_2$, and 1% bovine serum albumin were incubated with the primary antibody of 5 μg/ml of a mouse monoclonal antibody (mAb) specific for αIIbβ3, HIP8 (BD Biosciences) for 30 minutes at 4°C. After washing, the cells were incubated with the secondary Ab of ~1 μg/ml phycoerythrin (PE)-conjugated rat anti-mouse IgG (BD Biosciences) for 30 minutes at 4°C, washed once, stained with 1 μg/ml 7-aminoactinomycin D (7AAD) (Sigma-Aldrich) to discriminate dead cells, and then analyzed on a flow cytometer (FACSCalibur; BD Biosciences). As a negative control, cells were incubated with the secondary Ab alone. For the binding of a ligand-mimetic, activation-specific anti-αIIbβ3 mAb, PAC-1 (BD Biosciences), cells were incubated with 10 μg/ml PAC-1 for 30 minutes at room temperature in the absence or presence of 10 μM of a peptidomimetic antagonist of αIIbβ3, Ro44-9883 (a gift from Astellas Pharma, Tokyo, Japan), washed once, and then incubated with 10 μg/ml PE-conjugated anti-mouse IgM (eBioscience, San Diego, CA) for 30 minutes at 4°C. After washing, cells were stained with 7AAD and then analyzed. As a positive control for PAC-1 binding, cells were incubated with 15 mM dithiothreitol (DTT) for 10 minutes at 37°C to activate integrin αIIbα6Bβ3 and incubated with PAC-1 as mentioned above. Integrin activation was quantified as an activation index calculated using the following formula: 100 x (F − Fo) / (Fmax − Fo), where F is the median fluorescence intensity (MFI) of PAC-1 binding, Fo is the PAC-1 binding in the presence of Ro44-9883, and Fmax is the maximal PAC-1 binding in the cells treated with DTT. For fibrinogen binding, cells were incubated with 150 μg/ml Alexa-Fluor 647-conjugated fibrinogen (Molecular Probes, Eugene, OR) under similar conditions to the above assay. In some experiments using αIIbβ3-expressing CHO cells, the activation indexes were normalized by αIIbβ3 expression, as shown by the following formula: 100 x (F − Fo) / (F_1 - F_2), where F and Fo are the same as mentioned above, F_1 is the HIP8 binding, and F_2 is the binding of the secondary Ab alone.

Immunoblotting

Immunoblotting was performed using procedures previously described [31]. In brief, cell lysates were subjected to sodium dodecyl sulfate-polyacrylamide gel electrophoresis (SDS-PAGE) and transferred to a polyvinylidene difluoride (PVDF) membrane. The membranes were incubated with either one of the following primary Abs: 0.125 μg/ml mouse mAb specific for ILK, 3/ILK (BD Biosciences), 0.25 μg/ml mouse mAb specific for PINCH, 49/PINCH (BD Biosciences), rabbit polyclonal Ab specific for α-parvin (IgG fraction; 1:3,000) (Sigma-Aldrich), 1 μg/ml mouse mAb specific for β-parvin, 11A5 (Millipore, Temecula, CA), mouse mAb specific for talin, 8D4 (ascites fluid; 1:2,000) (Sigma-Aldrich), rabbit polyclonal Ab specific for kindlin-2 (IgG fraction; 1:1,000) (ProteinTech Group, Chicago, IL), 0.5 μg/ml rabbit polyclonal Ab specific for glyceraldehyde-3-phosphate dehydrogenase (GAPDH), FL-335 (Santa Cruz Biotechnology), horseradish peroxidase (HRP)-conjugated rabbit polyclonal Ab specific for β-actin (IgG fraction; 1:2000) (MBL, Woburn, MA), or 1 μg/ml mouse mAb specific for GFP, B-2 (Santa Cruz Biotechnology) for 90 minutes at room temperature. After washing, bound Abs except for the HRP-conjugated Abs were incubated with peroxidase-conjugated secondary Abs (Kirkegaard & Perry Labs, Gaithersburg, MD) Detection was performed using a chemiluminescence kit (Immobilon Western; Millipore, Bedford, MA). Chemiluminescence was visualized by an image analyzer, LAS-3000PLUS (Fuji Photo Film, Kanagawa, Japan).

Immunoprecipitation

Parental cells were solubilized at concentrations of 2 x 10^7 cells/ml in a lysis buffer (150 mM NaCl, 50 mM Tris-HCl, pH 7.5, and 1% Triton X-100) containing proteinase inhibitors. After centrifugation at 15,000 x g for 12 min, the supernatant (200 μl) was subjected to immunoprecipitation using protein A/G agarose (Santa Cruz Biotechnology) and the following Abs: 1 μg mouse mAb specific for ILK, 3/ILK, 1 μg mouse mAb specific for PINCH, 49/PINCH, 1 μg mouse IgG_1 isotype control, MOPC 21 (Sigma-Aldrich), 1 μg mouse IgG_{2a} isotype control, UPC-10 (Sigma-Aldrich), 1 μg rabbit polyclonal Ab specific for α-parvin, and 1 μg pooled rabbit IgG (Invitrogen). The immunoprecipitants were analyzed by immunoblotting as described above. As a positive control, cell lysates (15 μl) were loaded onto a lane.

Short interfering RNA (siRNA) and transfection

Total RNA from parental cells was extracted with Trizol reagent (Invitrogen). PINCH-1, α- and β-parvin, and kindlin-2 mRNA were amplified by a one-step RT-PCR kit (Qiagen, Valencia, CA) using primers specific to both mouse and rat homologues according to the manufacturer's instructions. RT-PCR products were directly sequenced using specific primers.

siRNAs against RNA targets were designed and synthesized by Invitrogen (Stealth RNAi). The siRNA target sequences of hamster mRNA are as follows: PINCH-1 (p) 157 sense 5'-CGGGUUAUUAAAGCCAUGAACAACA-3'; PINCH-1 (p) 755 sense 5'-CCTGCAATACCAAATTAACACTCAA-3'; α-pavin (pa) 503 sense 5'-CCAGGAGCATCAAGTGGAATGTAGA-3'; α-pavin (pa) 761 sense 5'-CAGACAAGCTCAACGTGGTAAAGAA-3'; β-pavin (pb) 900 sense 5'-UCCACAACUUCUACCUGACACCUGA-3'; β-pavin (pb) 1011 sense 5'-AAGAUGUGGUAAACUUGGACCUCAA-3'; kindlin-2 (k) 770 sense 5'-GAUCGCUAAUGGAACAAGAUGUGUGAA-3'; kindlin-2 (k) 770 scrambled control sense 5'-GAUAUCGUAAAGAACUAGUGCGGAA-3'; kindlin-2 (k) 1733 sense 5'-AAGGCGGCAAGAGAGAAGAACUUAU-3'; kindlin-2 (k) 1733 scrambled control sense 5'-AAGCGGGAAAGAAAGAAGUCGCUAU-3'. The sequences of ILK siRNA (Ilk1255) and its scrambled control were previously described [31]. Stealth RNAi-negative control duplexes (Invitrogen) were used as controls in knockdown experiments targeting PINCH-1 and parvins. Cells cultured in six-well plates were transfected with 12.5-50 nM siRNA using Lipofectamine RNAiMAX (Invitrogen) or cotransfected with 30 nM siRNA and the indicated amounts of plasmid (0.5 μg pEGFP-N1 encoding THD-fused GFP or 0.015 μg pEGFP-N1 plus 0.485 μg pcDNA3 as a negative control) using Lipofectamine 2000. Transfected cells were usually analyzed at 72 hours after transfection. For transfections with plasmid DNA alone, Lipofectamine 2000 was employed.

Statistical analysis

The statistical significance of observed data was determined using one-way analysis of variance followed by Bonferroni's post hoc test using PRISM 5 software (GraphPad Software; La Jolla, CA, USA). P values of 0.05 or less were considered statistically significant.

Results

Evaluation of PINCH, α-parvin, talin, and kindlin-2 in ILK-deficient αIIbα6Bβ3- inactive mutant CHO cells and αIIbα6Bβ3-active parental CHO cells

We previously obtained ILK-deficient mutant cells by treating parental cells expressing constitutively active αIIbα6Bβ3 with the chemical mutagen EMS [31]. In the mutant cells, ILK mRNAs contained two nonsense mutations, R317X and W383X, in a compound heterozygous state, resulting in a complete lack of ILK expression. It has been shown that ILK forms a ternary complex with PINCH and parvins to make an IPP complex [25]. To assess the role of ILK-binding proteins in ILK-deficient mutant cells with the inactive state of αIIbα6Bβ3, we examined the protein expression of ILK-binding adaptor proteins, PINCH and α-parvin. In addition to a lack of ILK expression, mutant cells showed severe reductions in the protein expression of PINCH and α-parvin as compared to parental cells. In contrast, talin and kindlin-2, which play critical roles in integrin activation, were present at normal levels of protein expression (Figure 1A). Transfection of a plasmid encoding ILK cDNA into mutant cells showed the increased expression of ILK and concomitant increases in PINCH and α-parvin expression levels but did not affect talin and kindlin-2 expression levels. Moreover, flow cytometry using an activation-specific anti-αIIbβ3 mAb, PAC-1, showed that ILK-plasmid transfection increased PAC-1 binding compared to empty-plasmid transfection (Figure 1B). These data suggest that ILK, PINCH, and α-parvin are necessary to restore the active state of αIIbα6Bβ3 in mutant cells.

Detection and assessment of ILK, PINCH, and parvin (IPP) complex in αIIbα6Bβ3-active parental cells

Since ILK, PINCH, and parvins form the IPP complex, we assessed IPP complex formation in αIIbα6Bβ3-active parental cells, which show constitutively active αIIbα6Bβ3. Immunoprecipitation experiments revealed that ILK is coprecipitated with PINCH and α-parvin, indicating the presence of the IPP complex in those cells (Figure 2). To evaluate the importance of these proteins comprising the complex on the active state of αIIbα6Bβ3, we performed RNA interference (RNAi) experiments targeting PINCH or parvins, and we analyzed the active state of αIIbα6Bβ3 by flow cytometry using PAC-1. For PINCH siRNA, we targeted PINCH-1, one of the two PINCH isoforms, because we failed to find sequences of PINCH-2 mRNA in CHO cells. Each of the two PINCH-1 siRNAs (p157 and p755) decreased PINCH expression and concomitantly decreased ILK and α-parvin expression compared to nontargeting negative control siRNA in parental cells (Figure 3A), leading to a decreased integrin activation index, which was determined by flow cytometry analysis of PAC-1 binding (Figure 3B). For parvin siRNA, α- and β-parvins were knocked down since both parvins are thought to bind to ILK. A mixture of two α-parvin siRNAs (pa503 and pa761) or two β-parvin siRNAs (pb900 and pb1011) reduced α-parvin or β-parvin expression, respectively; however, ILK and PINCH expression levels were less significantly affected (Figure 3C). When a mixture of α-parvin and β-parvin siRNAs was transfected into parental cells, the expression levels of α-parvin and β-parvin were decreased and concomitant decreases in ILK and PINCH expression were observed. Flow cytometry analysis evaluating the activation state exhibited that the transfection of both α- and β-parvin siRNAs, but not that of either α- or β-parvin siRNA significantly decreased PAC-1 binding (Figure 3D). These data suggest that the IPP complex formation of ILK, PINCH, and parvins is necessary for αIIbα6Bβ3 activation in a CHO cell system.

Knockdown of kindlin-2 in αIIbα6Bβ3-active parental cells

In our previous work, talin siRNA decreased PAC-1 binding to αIIbα6Bβ3-active parental cells [31]. To confirm that kindlin-2 plays an important role in integrin activation in the CHO cell system, we performed the kindlin-2 siRNA experiment in parental cells (Figure 3E, F). Each of two different siRNAs (k770 and k1733) reduced kindlin-2 expression and decreased PAC-1 binding in association without significantly affecting ILK or talin expression. In addition, when an ILK cDNA was cotransfected with kindlin-2 siRNA into ILK-deficient mutant

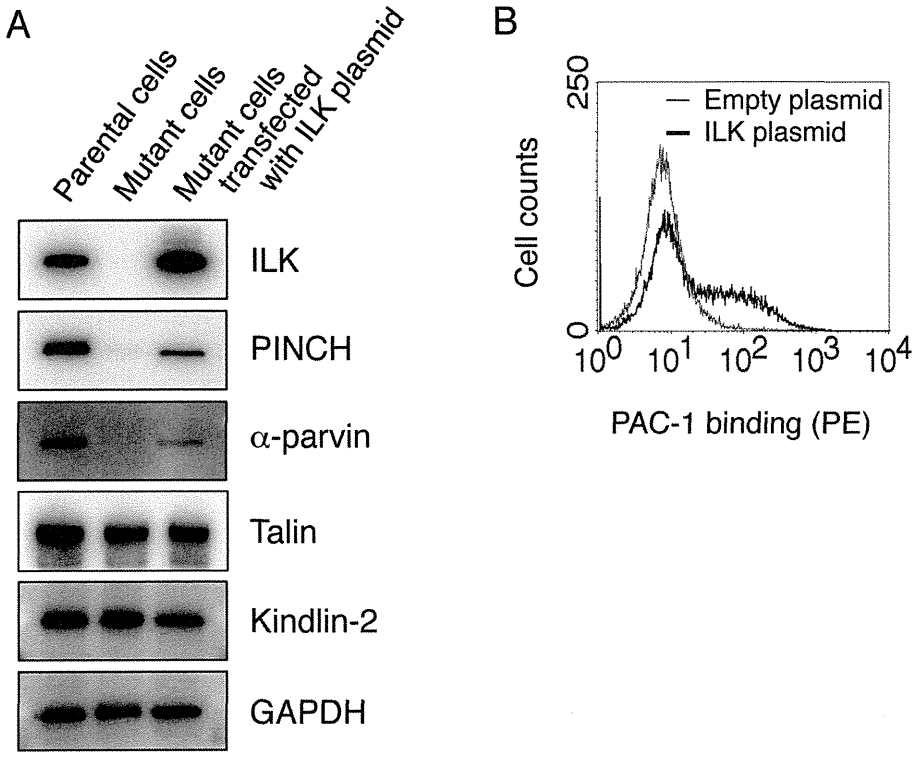

Fig. 1

Figure 1. Characterization of ILK-deficient mutant cells expressing inactive αIIbα6Bβ3. (A) Immunoblotting for ILK, PINCH, α-parvin, talin, and kindlin-2. Cell lysates obtained from parental cells with constitutively active αIIbα6Bβ3, ILK-deficient mutant cells with inactive αIIbα6Bβ3, and mutant cells transiently transfected with rat ILK cDNA were electrophoresed on SDS-PAGE gels and immunoblotted with indicated Abs. GAPDH shows an internal loading control. (B) Flow cytometry analysis showing PAC-1 (an activation-specific mAb for αIIbβ3) binding to mutant cells transiently transfected with either ILK plasmid or empty plasmid. Bound PAC-1 was detected with a PE-conjugated secondary mAb.

doi: 10.1371/journal.pone.0085498.g001

cells, PAC-1 binding was decreased as compared to those of the cotransfection of both the ILK cDNA and scrambled kindlin-2 siRNA (data not shown). These data indicate that kindlin-2 is required for αIIbα6Bβ3 activation in parental cells.

Role in binding of ILK to PINCH and parvin for integrin activation

To examine the significance of ILK-PINCH binding for integrin activation, we generated a GFP-fused ILK mutant (GFPILK-H99D/F109A/W110A) in which mutations were introduced into the binding sites for the LIM1 domain of PINCH in the ankyrin repeat domain of ILK. This ILK mutant is designed to disrupt ILK-PINCH binding but not ILK-α-parvin binding. When GFPILK-WT cDNA was transfected into mutant cells, PAC-1 binding was increased (Figure 4A). Transfection of the GFPILK-H99D/F109A/W110A cDNA into mutant cells failed to recover PAC-1 binding and did not induce an obvious upregulation of PINCH expression, whereas the ILK mutant protein was well expressed and α-parvin was similarly increased compared to the case with GFPILK-WT cDNA transfection, indicating the ILK-α-parvin complex (Figure 4B). These data suggest that ILK-PINCH binding is required for stable PINCH expression even in the presence of ILK, as well as for αIIbα6Bβ3 activation in the CHO cell system. When cell lysates of the mutant cells transfected with the GFPILK-H99D/F109A/W110A cDNA was subjected to immunoprecipitation with anti-α-parvin Ab, the ILK mutant was coprecipitated (data not shown). In addition, we generated a GFP-fused ILK mutant (GFPILK-M402A/K403A) that disrupts the parvin binding and that impairs the localization of ILK to focal adhesions as shown in the previous report [35]. Transfection of GFPILK-M402A/K403A cDNA into mutant cells showed strongly impaired PAC-1 binding and did not induce an overt upregulation of α-parvin expression (Figure 4C, D). These data suggest that ILK-parvin binding is necessary for stable parvin expression, as well as for αIIbα6Bβ3 activation in the CHO cell system.

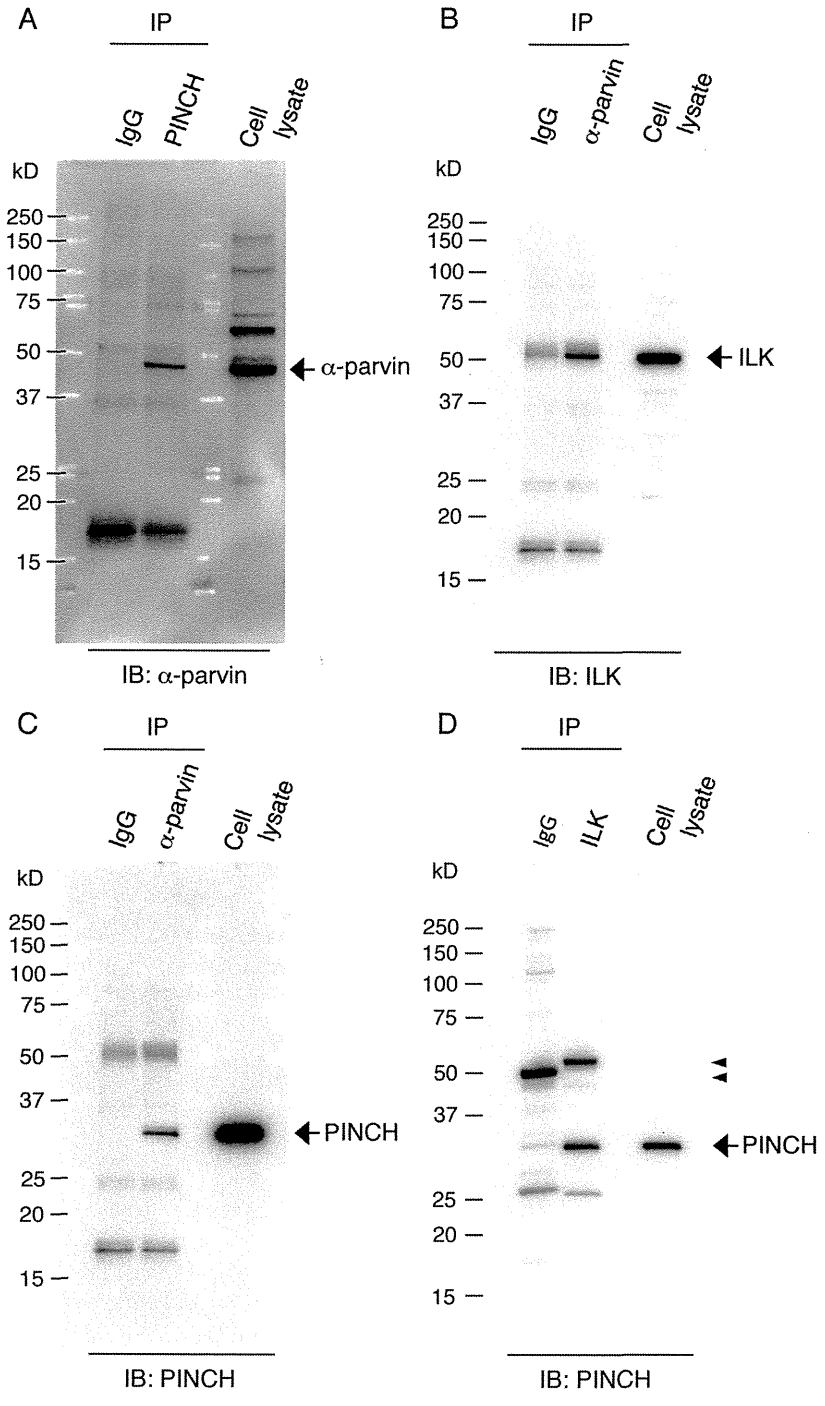

Fig. 2

Figure 2. Detection of IPP complex proteins in αIIbα6Bβ3-active parental cells. Cell lysates obtained from αIIbα6Bβ3-active parental cells were immunoprecipitated with Abs against PINCH (A), α-parvin (B, C), and ILK (D). The co-precipitates were detected by Abs for α-parvin (A), ILK (B), and PINCH (C, D). IgG means immunoprecipitation (IP) using non-immune control IgG. IB stands for immunoblotting. Arrows indicate the predicted sizes of the indicated proteins. Arrowheads (D) indicate the antibody heavy chains used in the IP. Different mobilities between those of the two IgG antibodies are probably caused by differences in the amino acid compositions of them.

doi: 10.1371/journal.pone.0085498.g002

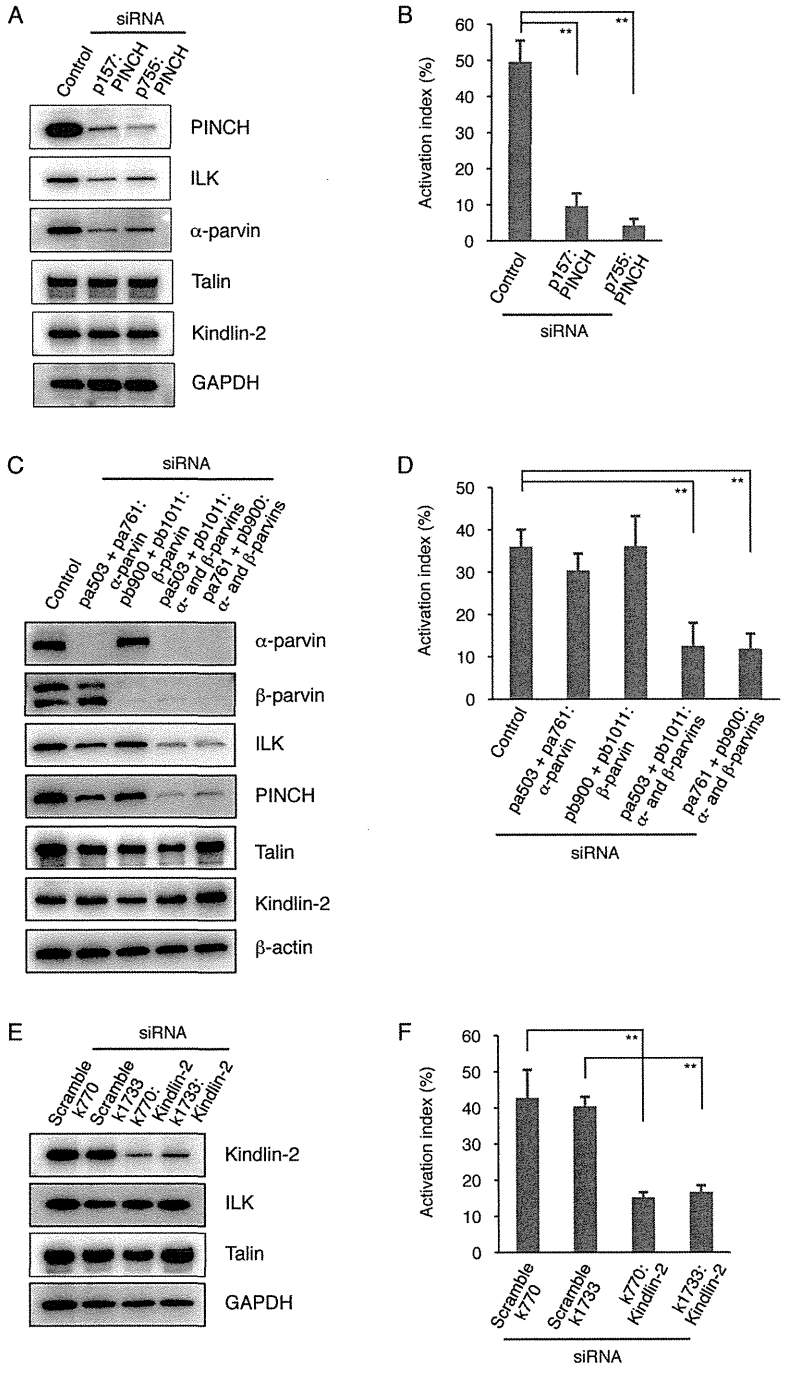

Fig. 3

Figure 3. Knockdown effects of PINCH, parvins, and kindlin-2 in αIIbα6Bβ3-active parental cells. αIIbα6Bβ3-active parental cells were transiently transfected with PINCH siRNAs (p157 and p755) (A), α-parvin siRNAs (pa503 and pa761) (C), β-parvin siRNAs (pb900 and pb1011) (C), kindlin-2 siRNAs (k770 and k1733) (E), negative control siRNAs, and scrambled siRNAs. Cell lysates were electrophoresed on SDS-PAGE gels, and the separated proteins were immunoblotted with the indicated Abs. GAPDH and β-actin are shown as internal loading controls. The activation indexes of transfected cells (B, D, F) were calculated using the formula shown in Materials and Methods. A value of 100% implies the maximum PAC-1 binding to the cells treated with dithiothreitol (DTT). Data represent means ± standard deviation (SD) of three (B, F) or four (D) independent experiments. ** indicates $P < 0.01$.

doi: 10.1371/journal.pone.0085498.g003

Moreover, when fibrinogen, a natural ligand for αIIbβ3, was used instead of PAC-1 in these experiments, similar results were obtained (Figure 4E).

Analysis of ILK in inactive αIIbβ3-expressing CHO cells

αIIbβ3 is present in an inactive state on CHO cells, and overexpression of the THD into those cells can induce αIIbβ3 activation [36]. The THD directly binds the integrin β3 cytoplasmic domain and causes integrin activation. To examine ILK's contribution to THD-mediated αIIbβ3 activation, we performed knockdown experiments targeting ILK under transient THD expression (Figure 5). For the cotransfection of THD-GFP cDNA with scrambled ILK siRNA (scramble Ilk1255), the THD-GFP highly expressing cells exhibited a significant increase in the PAC-1 binding as compared to the case with GFP cDNA cotransfection (Figure 5A, B). In contrast, the cotransfection of THD-GFP cDNA with ILK siRNA (Ilk1255) showed decreased PAC-1 binding in the cells with high expression of THD-GFP (Figure 5A, B). The protein expression levels of ILK, PINCH, and α-parvin were suppressed by the cotransfection of ILK siRNA and THD-GFP cDNA, whereas the expression level of THD-GFP was not changed in the presence of ILK siRNA (Figure 5C). These results suggest that THD is sufficient to restore partially the integrin activation upon elimination of ILK by its siRNA (Ilk1255) and that ILK may assist THD in regulating the integrin activation state by assembling the IPP complex. In addition, these findings obtained from αIIbβ3-expressing CHO cells support the importance of the IPP complex observed in the αIIbα6Bβ3-expressing CHO cells. □

Overexpression of the IPP complex in inactive αIIbβ3-expressing CHO cells

To examine the IPP complex's role in THD-mediated αIIbβ3 activation, we performed overexpression experiments of ILK, PINCH-1, and α-parvin in inactive αIIbβ3-expressing CHO cells. As expected, THD-GFP overexpression into αIIbβ3-expressing CHO cells induced PAC-1 binding in the cells with high expression of THD-GFP, as compared to the case with GFP cDNA transfection (Figure 6A, B). Interestingly, although quadruple overexpression of GFP and IPP did not significantly increase PAC-1 binding, quadruple overexpression of THD-GFP and IPP caused higher PAC-1 binding compared to the case with THD-GFP overexpression, suggesting a supportive effect of IPP on THD-mediated αIIbβ3 activation (Figure 6A, B). Kindlin-2 binds to the integrin β3 cytoplasmic domain and functions as a co-activator of talin [12,37]. As expected, double overexpression of THD-GFP and kindlin-2 cooperatively increased PAC-1 binding (Figure 6A, B), suggesting that both THD and kindlin-2 are required for the full activation of αIIbβ3. Regarding protein expression, THD-GFP was adequately expressed in each transfection, and the expression levels of ILK, PINCH, α-parvin, and kindlin-2 were higher than their endogenous expression levels in the cells with indicated transfection (Figure 6C). Thus, these data suggest that the IPP complex supports the THD for integrin αIIbβ3 activation.

Discussion

ILK is a multidomain scaffold protein that interacts with several cytoplasmic proteins [38,39]. In integrin adhesion sites, ILK exists in a ternary complex composed of the two other proteins PINCH and parvin. The ternary complex formation can stabilize each component and exert its function. In fact, ILK-deficient mutant CHO cells exhibited profoundly reduced PINCH and α-parvin expression levels, leading to inactive αIIbα6Bβ3 (Figure 1). The introduction of ILK expression into ILK-deficient mutant cells increased the expression levels of PINCH and α-parvin, accompanied by αIIbα6Bβ3 activation (Figure 1). The involvement of the IPP complex formation in integrin activation was confirmed in the knockdown experiments of PINCH and parvins in αIIbα6Bβ3-active parental cells (Figure 3). The ILK mutants with defects in either PINCH or parvin binding did not activate αIIbα6Bβ3 in ILK-deficient mutant cells (Figure 4). Since it has been reported that the parvin-binding defective ILK mutant (M402A/K403A) fails to localize to focal adhesions [35], these two ILK mutants are probably not recruited to the αIIbα6Bβ3 sites in a process of integrin activation. Thus, our data support a previous report that the proper complex formation of ILK, PINCH, and parvin is necessary for ILK recruitment to the integrin adhesion sites [35,40].

Recent studies of integrin regulatory proteins have shown that both talin and kindlins directly bind to different regions in the integrin β cytoplasmic domain and cooperate in a final step of integrin activation [9,12]. In our experiments, kindlin-2 knockdown in αIIbα6Bβ3-active parental cells reduced the activation state of αIIbα6Bβ3, and talin knockdown exhibited similar results in our previous work [31]. The knockdown of PINCH and of parvins in the IPP complex decreased the activation state of αIIbα6Bβ3 in parental cells to a similar extent as did the knockdown of either kindlin-2 or talin. In inactive αIIbβ3-expressing CHO cells, overexpression of THD-GFP induced αIIbβ3 activation, and ILK knockdown reduced THD-GFP-mediated αIIbβ3 activation (Figure 5). Moreover, overexpression of the IPP complex further augmented the activation state of αIIbβ3 induced by the THD in inactive αIIbβ3-expressing CHO cells (Figure 6). These data suggest that the IPP complex participates in the cooperation of talin and kindlin-2 during the activation processes of not only αIIbα6Bβ3 but also αIIbβ3. The precise binding sites of ILK in the integrin β cytoplasmic domain remain to be determined, although their interaction has been reported [19]. There seem to be two possible direct and indirect manners of ILK binding to the integrin cytoplasmic domain. It was recently reported that the binding of PAT-4 (ILK) to UNC-112 (kindlin) in *C. elegans* is necessary for UNC-112 recruitment to adhesion sites [41]. While kindlin alone appears to bind to integrin in mammalian cells, the IPP complex would contribute to effective binding of kindlin to the β integrin cytoplasmic domain to fully induce conformational changes of integrin.

Adaptor proteins, PINCH-1 and -2, share high amino acid sequence identity [27]. Those are ubiquitously expressed in different tissues and show overlapping expression in many tissues. Both isoforms bind equally well to ILK, but its binding is

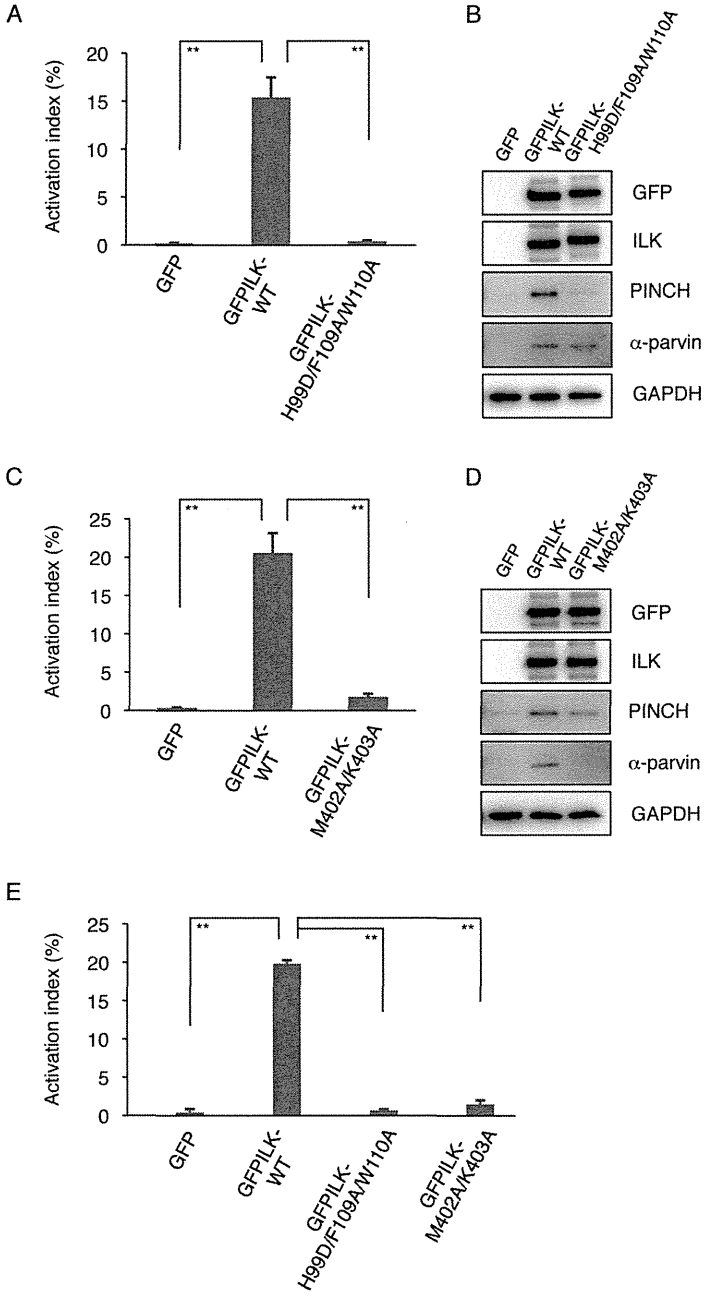

Fig.4

Figure 4. Effects of ILK mutants with defects in either PINCH or parvin binding. The activation indexes of transfected cells (A, C, E). ILK-deficient mutant cells were transiently transfected with GFP cDNA, GFP-fused wild-type ILK (GFPILK-WT) cDNA, GFP-fused ILK mutant with defective PINCH binding (GFPILK-H99D/F109A/W110A) cDNA (A, E), or GFP-fused ILK mutant with defective parvin binding (GFPILK-M402A/K403A) cDNA (C, E). After transfection, the binding of either PAC-1 (A, C) or fibrinogen (E) to the cells was analyzed by flow cytometry. The activation index was determined by the formula shown in Materials and Methods. A value of 100% represents the maximal binding of PAC-1 or fibrinogen to the cells treated with dithiothreitol. Data represent means ± SD of three independent experiments. ** indicates $P < 0.01$. Immunoblotting showing protein expression of GFP (B, D), GFP-fused wild-type ILK (GFPILK-WT) (B, D), GFP-fused ILK mutant with defective PINCH binding (GFPILK-H99D/F109A/W110A) (B), and GFP-fused ILK mutant with defective parvin binding (GFPILK-M402A/K403A) (D) in ILK-deficient mutant cells. Cell lysates were electrophoresed and immunoblotted with indicated Abs.

doi: 10.1371/journal.pone.0085498.g004

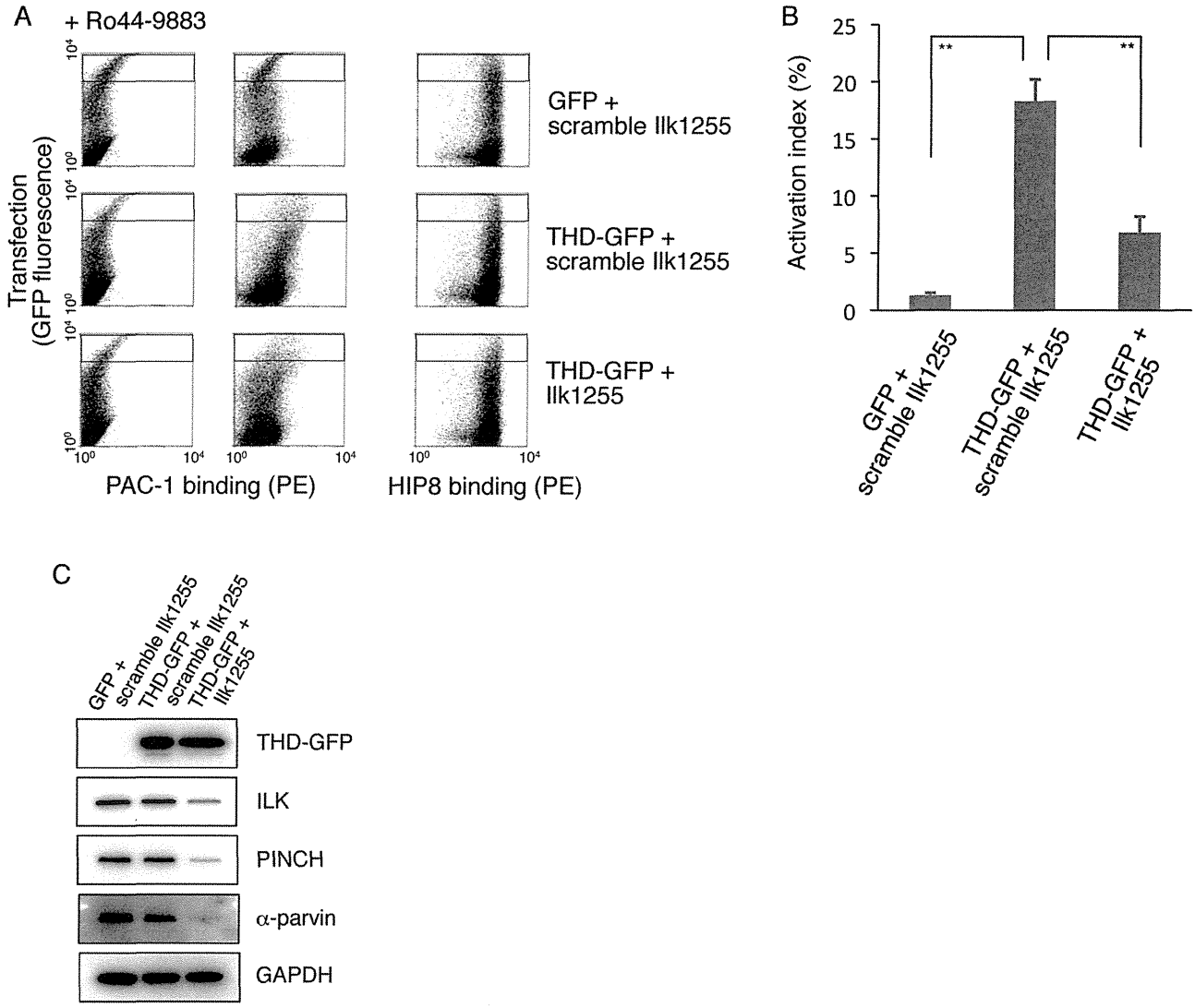

Fig. 5

Figure 5. Knockdown effects of ILK on THD-mediated αIIbβ3 activation. (A) Dot plot detecting PAC-1 binding to cotransfected cells. Inactive αIIbβ3-expressing CHO cells were transiently cotransfected with GFP cDNA plus scrambled ILK siRNA (scramble Ilk1255), with THD-GFP cDNA plus scrambled ILK siRNA (scramble Ilk1255), or with THD-GFP cDNA plus ILK siRNA (Ilk1255). Highly transfected cells (cells in gated regions) were analyzed for PAC-1 binding or HIP8 (an αIIbβ3-specific mAb) binding. (B) The activation indexes of transfected cells. The activation index was determined by the formula shown in Materials and Methods. A value of 100% implies the median fluorescence intensity of HIP8 binding to the cells in gated regions. Data represent means ± SD of three independent experiments. ** indicates $P < 0.01$. (C) Immunoblotting to evaluate expression levels of IPP and THD-GFP. Cell lysates were electrophoresed and immunoblotted with indicated Abs.

doi: 10.1371/journal.pone.0085498.g005

mutually exclusive [34,42]. PINCH-1 is expressed in hematopoietic systems, and strong expression of it has been observed in megakaryocytes during fetal liver hematopoiesis [27]. PINCH-2 also joins in the IPP complex and contributes to the stabilization of individual proteins. We examined only PINCH-1 expression in CHO cells since we were unable to find PINCH-2 mRNA in parental CHO cells. Our knockdown experiment using PINCH-1-specific siRNA revealed the reduction of both ILK and α-parvin expression levels. In addition, published amino acid sequences of hamster PINCH-2

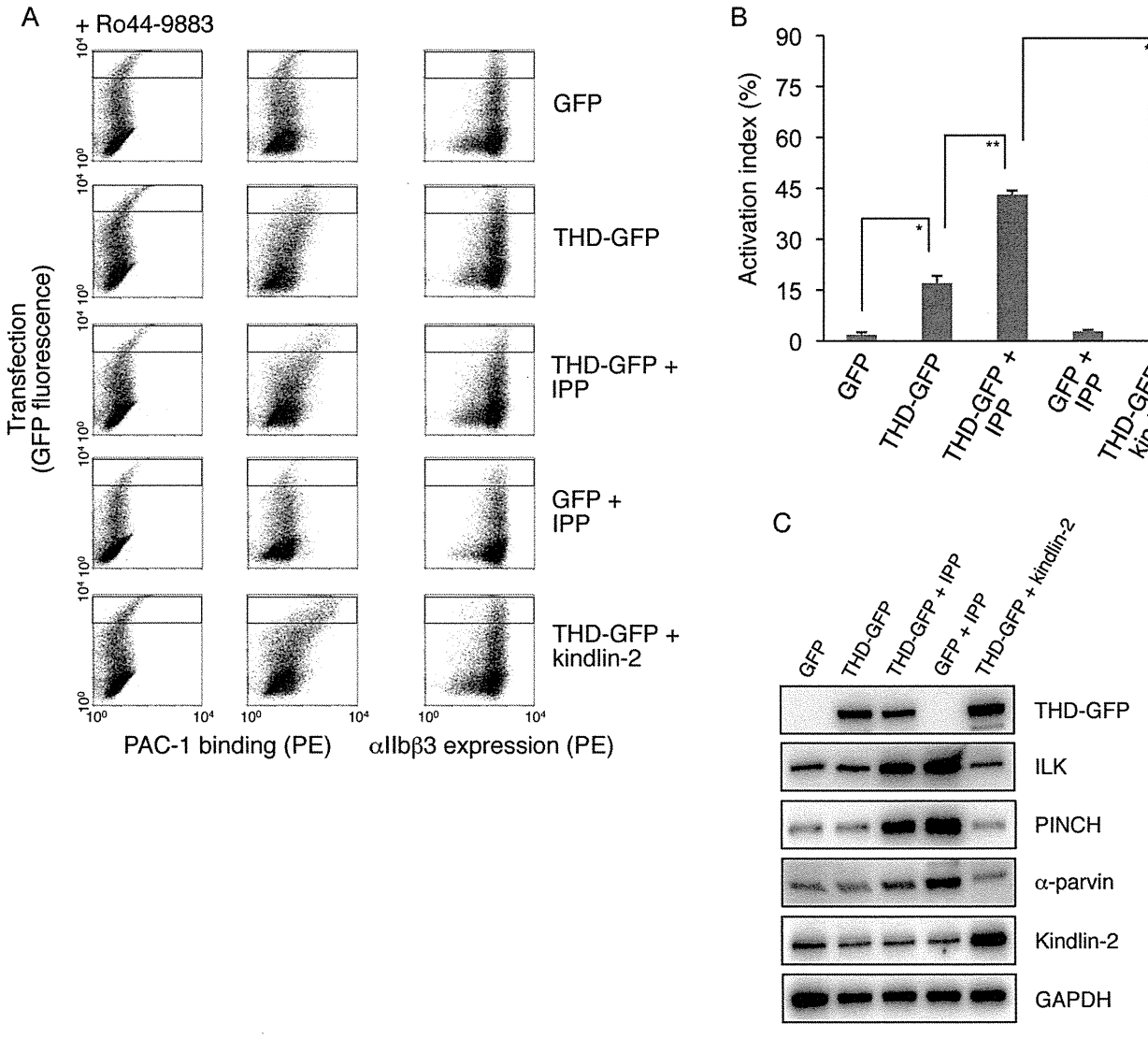

Fig. 6

Figure 6. Effects of IPP overexpression on THD-mediated integrin activation in inactive αIIbβ3-expressing CHO cells. (A) Dot plot detecting PAC-1 binding to transfected cells. Inactive αIIbβ3-expressing CHO cells were transiently transfected with GFP cDNA, with THD-GFP cDNA, with THD-GFP cDNA plus IPP (ILK, PINCH, and α-parvin) cDNAs, with GFP cDNA plus IPP cDNAs, or with THD-GFP cDNA plus kindling-2 cDNA. Highly transfected cells in the gated regions were analyzed for PAC-1 binding or HIP8 (an αIIbβ3-specific mAb) binding. (B) The activation indexes of transfected cells. The index was determined by the formula shown in Materials and Methods. A value of 100% implies the median fluorescence intensity of HIP8 binding to the cells in gated regions. Data represent means ± SD of three independent experiments. * and ** indicate $P < 0.05$ and $P < 0.01$, respectively. (C) Immunoblotting to evaluate expression levels of IPP, THD-GFP, and kindlin-2. Cell lysates obtained from transfected cells were electrophoresed and immunoblotted with indicated Abs.

doi: 10.1371/journal.pone.0085498.g006

(GenBank accession number EGW10997) showed an amino acid length composed of 144 residues, shorter than that of mouse PINCH-2 (accession number NP659111) composed of 341 residues. This suggested that proper PINCH-2 may not be expressed in CHO cells. Unlike PINCH, α- and β-parvins were expressed in CHO cells and the knockdown of both parvins but

not either α- or β-parvin decreased ILK and PINCH expression to a similar extent as the parvins. Thus, the parvins are complemented with each other in the formation of the IPP complex, and either one seems to support integrin activation by maintaining the IPP complex.

Platelets are likely to have α- and β-parvins, and both parvins contribute to the formation of the IPP complex [43,44]. The functional importance of the IPP complex for platelet integrin regulation has not been fully elucidated. There are only a few reports in which the IPP complex stably exists to a similar extent between resting and stimulated platelets [43,44]. It has been shown in human platelets that ILK is activated and binds to the β subunit of αIIbβ3 and the integrin collagen receptor α2β1 after stimulation with thrombin, phorbol 12-myristrate 13-acetate, and collagen [45,46]. These processes seem to aggregation-dependently occur in αIIbβ3 or aggregation-independently arise in α2β1. In a recent study using an ILK-conditional knockout mouse, ILK-deficient platelets exhibited reduced abilities of aggregation, fibrinogen binding, and α-granule secretion [33]. The ILK-deficient platelets also showed decreased expression levels of PINCH and α-parvin, suggesting that the IPP complex is involved in the regulation of integrin affinity. In platelets, the IPP complex may be translocated from the cytoplasm to the integrin β cytoplasmic domain in response to agonist stimulation and may participate in the control of integrin affinity.

The important role of ILK as a signal regulatory protein has been well investigated. Most works demonstrated that ILK functions in outside-in signaling through integrins [20,25,26,47-50]. In the present study, we showed that ILK supports integrin activation by assembling the IPP complex in the CHO cells. This effect may occur through a process in which kindlin-2 recruits ILK to integrins [37,51]. The IPP complex may participate in the cooperation of talin and kindlins in a final step of integrin activation and stabilize the active conformation of integrin.

Acknowledgements

We thank Drs. Koichi Kokame, Masashi Akiyama (National Cerebral and Cardiovascular Center), and Hirokazu Kashiwagi (Department of Hematology and Oncology, Osaka University Graduate School of Medicine) for helpful discussion.

Author Contributions

Conceived and designed the experiments: SH ST YT TM. Performed the experiments: SH HSI. Analyzed the data: SH HSI ST YT TM. Wrote the manuscript: SH YT TM.

References

1. Hynes RO (2002) Integrins: bidirectional, allosteric signaling machines. Cell 110: 673-687. doi:10.1016/S0092-8674(02)00971-6. PubMed: 12297042.
2. Shattil SJ, Newman PJ (2004) Integrins: dynamic scaffolds for adhesion and signaling in platelets. Blood 104: 1606-1615. doi: 10.1182/blood-2004-04-1257. PubMed: 15205259.
3. Tadokoro S, Shattil SJ, Eto K, Tai V, Liddington RC et al. (2003) Talin binding to integrin beta tails: a final common step in integrin activation. Science 302: 103-106. doi:10.1126/science.1086652. PubMed: 14526080.
4. Shattil SJ, Kim C, Ginsberg MH (2010) The final steps of integrin activation: the end game. Nat Rev Mol Cell Biol 11: 288-300. doi: 10.1038/nrm2871. PubMed: 20308986.
5. Calderwood DA, Yan B, de Pereda JM, Alvarez BG, Fujioka Y et al. (2002) The phosphotyrosine binding-like domain of talin activates integrins. J Biol Chem 277: 21749-21758. doi:10.1074/jbc.M111996200. PubMed: 11932255.
6. Anthis NJ, Wegener KL, Ye F, Kim C, Goult BT et al. (2009) The structure of an integrin/talin complex reveals the basis of inside-out signal transduction. EMBO J 28: 3623-3632. doi:10.1038/emboj.2009.287. PubMed: 19798053.
7. Elliott PR, Goult BT, Kopp PM, Bate N, Grossmann JG et al. (2010) The Structure of the talin head reveals a novel extended conformation of the FERM domain. Structure 18: 1289-1299. doi:10.1016/j.str.2010.07.011. PubMed: 20947018.
8. Goult BT, Bouaouina M, Elliott PR, Bate N, Patel B et al. (2010) Structure of a double ubiquitin-like domain in the talin head: a role in integrin activation. EMBO J 29: 1069-1080. doi:10.1038/emboj.2010.4. PubMed: 20150896.
9. Moser M, Nieswandt B, Ussar S, Pozgajova M, Fässler R (2008) Kindlin-3 is essential for integrin activation and platelet aggregation. Nat Med 14: 325-330. doi:10.1038/nm1722. PubMed: 18278053.
10. Harburger DS, Bouaouina M, Calderwood DA (2009) Kindlin-1 and -2 directly bind the C-terminal region of beta integrin cytoplasmic tails and exert integrin-specific activation effects. J Biol Chem 284: 11485-11497. PubMed: 19240021.
11. Malinin NL, Plow EF, Byzova TV (2010) Kindlins in FERM adhesion. Blood 115: 4011-4017. doi:10.1182/blood-2009-10-239269. PubMed: 20228270.
12. Ma YQ, Qin J, Wu C, Plow EF (2008) Kindlin-2 (Mig-2): a co-activator of beta3 integrins. J Cell Biol 181: 439-446. doi:10.1083/jcb.200710196. PubMed: 18458155.
13. Moser M, Legate KR, Zent R, Fässler R (2009) The tail of integrins, talin, and kindlins. Science 324: 895-899. doi:10.1126/science.1163865. PubMed: 19443776.
14. Lee HS, Lim CJ, Puzon-McLaughlin W, Shattil SJ, Ginsberg MH (2009) RIAM activates integrins by linking talin to ras GTPase membrane-targeting sequences. J Biol Chem 284: 5119-5127. PubMed: 19098287.
15. Calderwood DA, Tai V, Di Paolo G, De Camilli P, Ginsberg MH (2004) Competition for talin results in trans-dominant inhibition of integrin activation. J Biol Chem 279: 28889-28895. doi:10.1074/jbc.M402161200. PubMed: 15143061.
16. Hughes PE, Renshaw MW, Pfaff M, Forsyth J, Keivens VM et al. (1997) Suppression of integrin activation: a novel function of a Ras/Raf-initiated MAP kinase pathway. Cell 88: 521-530. doi:10.1016/S0092-8674(00)81892-9. PubMed: 9038343.
17. Ramos JW, Kojima TK, Hughes PE, Fenczik CA, Ginsberg MH (1998) The death effector domain of PEA-15 is involved in its regulation of integrin activation. J Biol Chem 273: 33897-33900. doi:10.1074/jbc.273.51.33897. PubMed: 9852038.
18. Zent R, Fenczik CA, Calderwood DA, Liu S, Dellos M et al. (2000) Class- and splice variant-specific association of CD98 with integrin beta cytoplasmic domains. J Biol Chem 275: 5059-5064. doi:10.1074/jbc.275.7.5059. PubMed: 10671548.
19. Hannigan GE, Leung-Hagesteijn C, Fitz-Gibbon L, Coppolino MG, Radeva G et al. (1996) Regulation of cell adhesion and anchorage-dependent growth by a new beta 1-integrin-linked protein kinase. Nature 379: 91-96. doi:10.1038/379091a0. PubMed: 8538749.
20. Sakai T, Li S, Docheva D, Grashoff C, Sakai K et al. (2003) Integrin-linked kinase (ILK) is required for polarizing the epiblast, cell adhesion, and controlling actin accumulation. Genes Dev 17: 926-940. doi: 10.1101/gad.255603. PubMed: 12670870.
21. Hannigan GE, McDonald PC, Walsh MP, Dedhar S (2011) Integrin-linked kinase: not so 'pseudo' after all. Oncogene 30: 4375-4385. doi: 10.1038/onc.2011.177. PubMed: 21602880.
22. Qin J, Wu C (2012) ILK: a pseudokinase in the center stage of cell-matrix adhesion and signaling. Curr Opin Cell Biol 24: 607-613. doi: 10.1016/j.ceb.2012.06.003. PubMed: 22763012.

23. Li F, Zhang Y, Wu C (1999) Integrin-linked kinase is localized to cell-matrix focal adhesions but not cell-cell adhesion sites and the focal adhesion localization of integrin-linked kinase is regulated by the PINCH-binding ANK repeats. J Cell Sci 112 (24): 4589-4599.
24. Tu Y, Li F, Goicoechea S, Wu C (1999) The LIM-only protein PINCH directly interacts with integrin-linked kinase and is recruited to integrin-rich sites in spreading cells. Mol Cell Biol 19: 2425-2434. PubMed: 10022929.
25. Tu Y, Huang Y, Zhang Y, Hua Y, Wu C (2001) A new focal adhesion protein that interacts with integrin-linked kinase and regulates cell adhesion and spreading. J Cell Biol 153: 585-598. doi:10.1083/jcb.153.3.585. PubMed: 11331308.
26. Yamaji S, Suzuki A, Sugiyama Y, Koide Y, Yoshida M et al. (2001) A novel integrin-linked kinase-binding protein, affixin, is involved in the early stage of cell-substrate interaction. J Cell Biol 153: 1251-1264. doi:10.1083/jcb.153.6.1251. PubMed: 11402068.
27. Braun A, Bordoy R, Stanchi F, Moser M, Kostka GG et al. (2003) PINCH2 is a new five LIM domain protein, homologous to PINCHand localized to focal adhesions. Exp Cell Res 284: 239-250. PubMed: 12651156.
28. Chu H, Thievessen I, Sixt M, Lämmermann T, Waisman A et al. (2006) gamma-Parvin is dispensable for hematopoiesis, leukocyte trafficking, and T-cell-dependent antibody response. Mol Cell Biol 26: 1817-1825. doi:10.1128/MCB.26.5.1817-1825.2006. PubMed: 16479001.
29. Tu Y, Li F, Wu C (1998) Nck-2, a novel Src homology2/3-containing adaptor protein that interacts with the LIM-only protein PINCH and components of growth factor receptor kinase-signaling pathways. Mol Biol Cell 9: 3367-3382. doi:10.1091/mbc.9.12.3367. PubMed: 9843575.
30. Widmaier M, Rognoni E, Radovanac K, Azimifar SB, Fässler R (2012) Integrin-linked kinase at a glance. J Cell Sci 125: 1839-1843. doi:10.1242/jcs.093864. PubMed: 22637643.
31. Honda S, Shirotani-Ikejima H, Tadokoro S, Maeda Y, Kinoshita T et al. (2009) Integrin-linked kinase associated with integrin activation. Blood 113: 5304-5313. doi:10.1182/blood-2008-07-169136. PubMed: 19299337.
32. Friedrich EB, Liu E, Sinha S, Cook S, Milstone DS et al. (2004) Integrin-linked kinase regulates endothelial cell survival and vascular development. Mol Cell Biol 24: 8134-8144. doi:10.1128/MCB.24.18.8134-8144.2004. PubMed: 15340074.
33. Tucker KL, Sage T, Stevens JM, Jordan PA, Jones S et al. (2008) A dual role for integrin-linked kinase in platelets: regulating integrin function and alpha-granule secretion. Blood 112: 4523-4531. doi:10.1182/blood-2008-03-148502. PubMed: 18772455.
34. Chiswell BP, Stiegler AL, Razinia Z, Nalibotski E, Boggon TJ et al. (2010) Structural basis of competition between PINCH1 and PINCH2 for binding to the ankyrin repeat domain of integrin-linked kinase. J Struct Biol 170: 157-163. doi:10.1016/j.jsb.2009.12.002. PubMed: 19963065.
35. Fukuda K, Gupta S, Chen K, Wu C, Qin J (2009) The pseudoactive site of ILK is essential for its binding to alpha-Parvin and localization to focal adhesions. Mol Cell 36: 819-830. doi:10.1016/j.molcel.2009.11.028. PubMed: 20005845.
36. Calderwood DA, Zent R, Grant R, Rees DJ, Hynes RO et al. (1999) The Talin head domain binds to integrin beta subunit cytoplasmic tails and regulates integrin activation. J Biol Chem 274: 28071-28074. doi:10.1074/jbc.274.40.28071. PubMed: 10497155.
37. Montanez E, Ussar S, Schifferer M, Bösl M, Zent R et al. (2008) Kindlin-2 controls bidirectional signaling of integrins. Genes Dev 22: 1325-1330. doi:10.1101/gad.469408. PubMed: 18483218.
38. Legate KR, Montañez E, Kudlacek O, Fässler R (2006) ILK, PINCH and parvin: the tIPP of integrin signalling. Nat Rev Mol Cell Biol 7: 20-31. doi:10.1038/nrm1789. PubMed: 16493410.
39. McDonald PC, Fielding AB, Dedhar S (2008) Integrin-linked kinase--essential roles in physiology and cancer biology. J Cell Sci 121: 3121-3132. doi:10.1242/jcs.017996. PubMed: 18799788.
40. Zhang Y, Guo L, Chen K, Wu C (2002) A critical role of the PINCH-integrin-linked kinase interaction in the regulation of cell shape change and migration. J Biol Chem 277: 318-326. PubMed: 11694512.
41. Qadota H, Moerman DG, Benian GM (2012) A molecular mechanism for the requirement of PAT-4 (integrin-linked kinase (ILK)) for the localization of UNC-112 (Kindlin) to integrin adhesion sites. J Biol Chem 287: 28537-28551. doi:10.1074/jbc.M112.354852. PubMed: 22761445.
42. Zhang Y, Chen K, Guo L, Wu C (2002) Characterization of PINCH-2, a new focal adhesion protein that regulates the PINCH-1-ILK interaction, cell spreading, and migration. J Biol Chem 277: 38328-38338. doi:10.1074/jbc.M205576200. PubMed: 12167643.
43. Yamaji S, Suzuki A, Kanamori H, Mishima W, Takabayashi M et al. (2002) Possible role of ILK-affixin complex in integrin-cytoskeleton linkage during platelet aggregation. Biochem Biophys Res Commun 297: 1324-1331. doi:10.1016/S0006-291X(02)02381-1. PubMed: 12372433.
44. Dittrich M, Birschmann I, Mietner S, Sickmann A, Walter U et al. (2008) Platelet protein interactions: map, signaling components, and phosphorylation groundstate. Arterioscler Thromb Vasc Biol 28: 1326-1331. doi:10.1161/ATVBAHA.107.161000. PubMed: 18451328.
45. Pasquet JM, Noury M, Nurden AT (2002) Evidence that the platelet integrin alphaIIb beta3 is regulated by the integrin-linked kinase, ILK, in a PI3-kinase dependent pathway. Thromb Haemost 88: 115-122. PubMed: 12152651.
46. Stevens JM, Jordan PA, Sage T, Gibbins JM (2004) The regulation of integrin-linked kinase in human platelets: evidence for involvement in the regulation of integrin alpha 2 beta 1. J Thromb Haemost 2: 1443-1452. doi:10.1111/j.1538-7836.2004.00870.x. PubMed: 15304053.
47. Attwell S, Mills J, Troussard A, Wu C, Dedhar S (2003) Integration of cell attachment, cytoskeletal localization, and signaling by integrin-linked kinase (ILK), CH-ILKBP, and the tumor suppressor PTEN. Mol Biol Cell 14: 4813-4825. doi:10.1091/mbc.E03-05-0308. PubMed: 12960424.
48. Grashoff C, Aszódi A, Sakai T, Hunziker EB, Fässler R (2003) Integrin-linked kinase regulates chondrocyte shape and proliferation. EMBO Rep 4: 432-438. doi:10.1038/sj.embor.embor801. PubMed: 12671688.
49. Terpstra L, Prud'homme J, Arabian A, Takeda S, Karsenty G et al. (2003) Reduced chondrocyte proliferation and chondrodysplasia in mice lacking the integrin-linked kinase in chondrocytes. J Cell Biol 162: 139-148. doi:10.1083/jcb.200302066. PubMed: 12835312.
50. Vouret-Craviari V, Boulter E, Grall D, Matthews C, Van Obberghen-Schilling E (2004) ILK is required for the assembly of matrix-forming adhesions and capillary morphogenesis in endothelial cells. J Cell Sci 117: 4559-4569. doi:10.1242/jcs.01331. PubMed: 15316070.
51. Chen K, Tu Y, Zhang Y, Blair HC, Zhang L et al. (2008) PINCH-1 regulates the ERK-Bim pathway and contributes to apoptosis resistance in cancer cells. J Biol Chem 283: 2508-2517. PubMed: 18063582.